FINAL REPORT
THE APPLICABILITY OF THE WEAP-86 PILE CAPACITY PREDICTION METHOD FOR CONNECTICUT SOILS
and
BEHAVIOR OF A SHEETPILE WALL FOR STABILIZATION OF A SLOPE IN PORTLAND

Project 86-7

by

Richard P. Long, Professor
Kenneth R. Demars, Assoc. Professor
William A. Shaheen, Grad. Student
Viroj Mekagaroon, Grad. Student

JHR 88-181 October 1988

This research was sponsored by the Joint Highway Research Advisory Council of the University of Connecticut and the Connecticut of the University of Connecticut and the Connecticut Department of Transportation, and was carried out in the Civil Engineering Department of the University of Connecticut.

Table of Contents

Introduction

The engineer requires reliable methods for predicting the capacity of piles as driven in the field. Early approaches used semi-empirical methods for making these predictions. The success of these early attempts was mixed. The Federal Highway Administration sponsored research to develop better methods for predicting pile capacity and a method evolved based on the work of Smith (1962) using the wave equation analogy as a means of modelling the pile driving operation and the resulting capacity of the pile. All mathematical models must be calibrated to field conditions in an area. The Connecticut Department of Transportation has conducted many load tests on piles over the years. In this phase of the project, pile capacity as predicted by WEAP was compared to the capacity measured by field load tests.

Scope of the Research

This phase of the research compares the pile capacity predicted by the WEAP-86 version of the Wave Equation Analysis of Piles (FHWA) to available appropriate pile load test results. Included in this project are the comparison of capacities for both monotube piles which develop their resistance through skin friction and H-Piles in glacial till whose capacity appears to be end bearing. The Soils and Foundation Division of ConnDOT made the results of 240 pile load tests available for comparison. These tests were screened for suitability for this investigation and many had to be excluded. The most common reasons for excluding individual tests from consideration were: The pile was not loaded to failure or that the pile was driven to bear on rock.

Field load tests are often "proof" tests to demonstrate that the pile as driven, can withstand at least twice the design load without excessive settlement. In these tests the ultimate capacity is not determined and a comparison with a predicted value from WEAP can not be made. When a pile is driven to rock, the load test shows primarily the elastic shortening of the pile and yields no useful information on the soil pile interaction properties.

After reviewing available test data, seven steel H-piles ranging in size from HP 10 x 42 through HP 12 x 74 were selected for comparison. The test data for the seven selected monotube piles indicated that their ultimate capacity depended on skin-friction together with an end-bearing component. Comparisons of field tests and WEAP were made for these piles.

An example of the load tests used in this investigation is shown in Fig. 1. The pile shown in Fig. 1 is an end-bearing pile driven into glacial till. The pile size is HP 12x74.

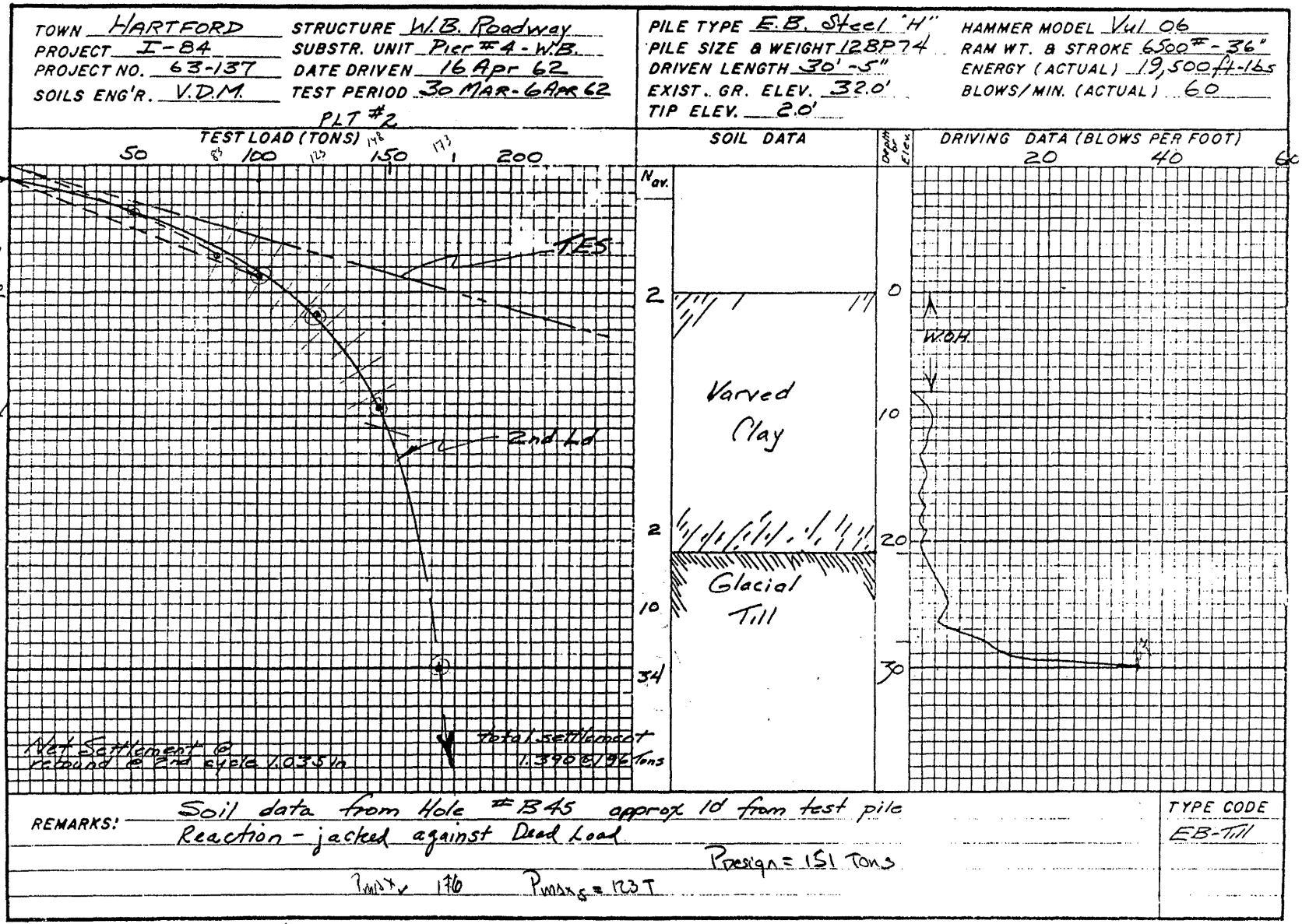

Figure 1. Typical End-Bearing H-Pile

Background

Pile foundation design requires prediction of both pile capacity and the length of pile. Prediction of the ultimate bearing capacity of pile may use two approaches; static analysis and dynamic analysis. The static analysis estimates capacity from soil properties with little regard to the manner by which the pile is placed, whereas the dynamic approach uses conservation of energy principles without regard to soil properties and behavior. Each approach has inherent advantages and disadvantages.

The static analysis requires accurate soil strength, soil unit weight, pore pressure information, and lateral earth pressure coefficients, together with pile dimensions to accurately predict pile capacity. The soil information is usually estimated from the boring logs. The problems involved with static analyses have led to the widespread use of simplistic energy-based formulas which do not consider soil properties in their development.

Dynamic analyses are based on equating the energy transferred to the pile by the hammer to the work done by the pile in penetrating the soil a finite distance. The penetration distance is called the set. This approach is attractive since the set can be observed in the field and used to control capacity. However, the physical properties of the pile and properties of the soil are not considered in early dynamic formulations. The first such formula appeared in Engineering News Record magazine and hence is known as the ENR formula. The original ENR equation to calculate the ultimate pile load (Pu) as a function of the final pile set is given by:

$$Pu = \frac{Wr \quad h}{s + 1}$$

where: Wr = weight of ram (kips)

h = height of fall (inches)

s = final pile set (inches)

The nominal factor of safety for this approach is 6 but field tests have frequently shown that the actual factor of safety by this equation can be less than 1, or greater than 6. Even though the ENR formula is one of the most unreliable methods available to predict Pu, it is still widely used to control pile driving due to its simplicity.

Soon after the development of the ENR formula, many others developed dynamic formulas for predicting Pu. Among the available formulas, the Hiley equation, and the Rational pile formula appear to be most accurate. These equations were the first to introduce a term to account for soil stiffness. The Hiley equation is shown to be,

$$Pu = \frac{e\ Wr\ h}{s + (K1 + K2 + K3)} \quad \frac{Wr + n^2\ Wp}{Wr + Wp}$$

where: e = hammer efficiency

Wr = weight of ram

h = ram fall

s = final pile set

Wp = weight of pile

n = coefficient of restitution

k1 = capblock and pile cap stiffness

k2 = pile stiffness

k3 = elastic compression of soil

The k3 term is a first step from the early dynamic formulations to a more complete model. The Hiley and Rational formulas were the first to consider soil stiffness in an energy formulation. Application of the wave equation to pile driving yielded a model that allows for pile dimensions, variable soil stiffness along the pile profile, soil and soil damping, system losses, etc. This was to become known as the wave equation analysis of piles (WEAP).

The wave equation was first put into practical form by E.A.L. Smith[1] in 1962. The greatest advantage of the wave equation is that it attempts to account for variation in a large number of physical parameters for any particular pile driving case. It predicts ultimate pile capacity as a function of the final blow count, and estimates stresses in the pile that develop during driving.

The wave equation uses physical properties of the pile soil system, accounts for energy losses in the system; and in-situ pile driving information to predict static pile capacity.

The wave equation may be derived from consideration of the internal forces and motion produced on a segment of a freely-suspended elastic bar subjected to an impact at one end. The resulting 1-D equation is:

$$\frac{d^2U}{dt^2} = c^2 \frac{d^2U}{dx^2}$$

where c = longitudinal wave velocity

U = longitudinal displacement

x = longitudinal coordinate

t = time

This one-dimensional wave equation has been derived from the equations of motion as outlined in Kolsky[2], and has been solved in

closed analytical form by Pochhammer[3] for a homogenous 1-D bar embedded in an homogeneous elastic medium. Standard linear, isotropic, elastic material properties are assumed for Pochhammer's exact solution. In practice; however, viscous soil damping, variable pile cross-sections, and variable pile cushion stiffness considerations all make exact analytical solutions impractical if not impossible to solve in closed form.

In addition, for a pile with non-zero skin friction, the resistance of the surrounding soil must also be considered. Modifying the above equation yields:

$$\frac{d^2U}{dt^2} = c^2 \frac{d^2U}{dx^2} +/- R \text{ , where R is a soil resistance term.}$$

The WEAP-86 computer program uses a finite-difference numerical solution to solve the above modified equation.

The approach used by WEAP-86 was first developed by Smith to determine the pile-set (or blow count) for a given ultimate static pile load. The pile system is idealized as shown in Figure 2 and consists of the following elements.

1. A weight (ram) to which an initial velocity is imparted from the hammer.
2. A capblock (hammer cushion)
3. A pile cap (anvil)
4. A cushion block (for concrete piles)
5. The pile
6. The supporting soil

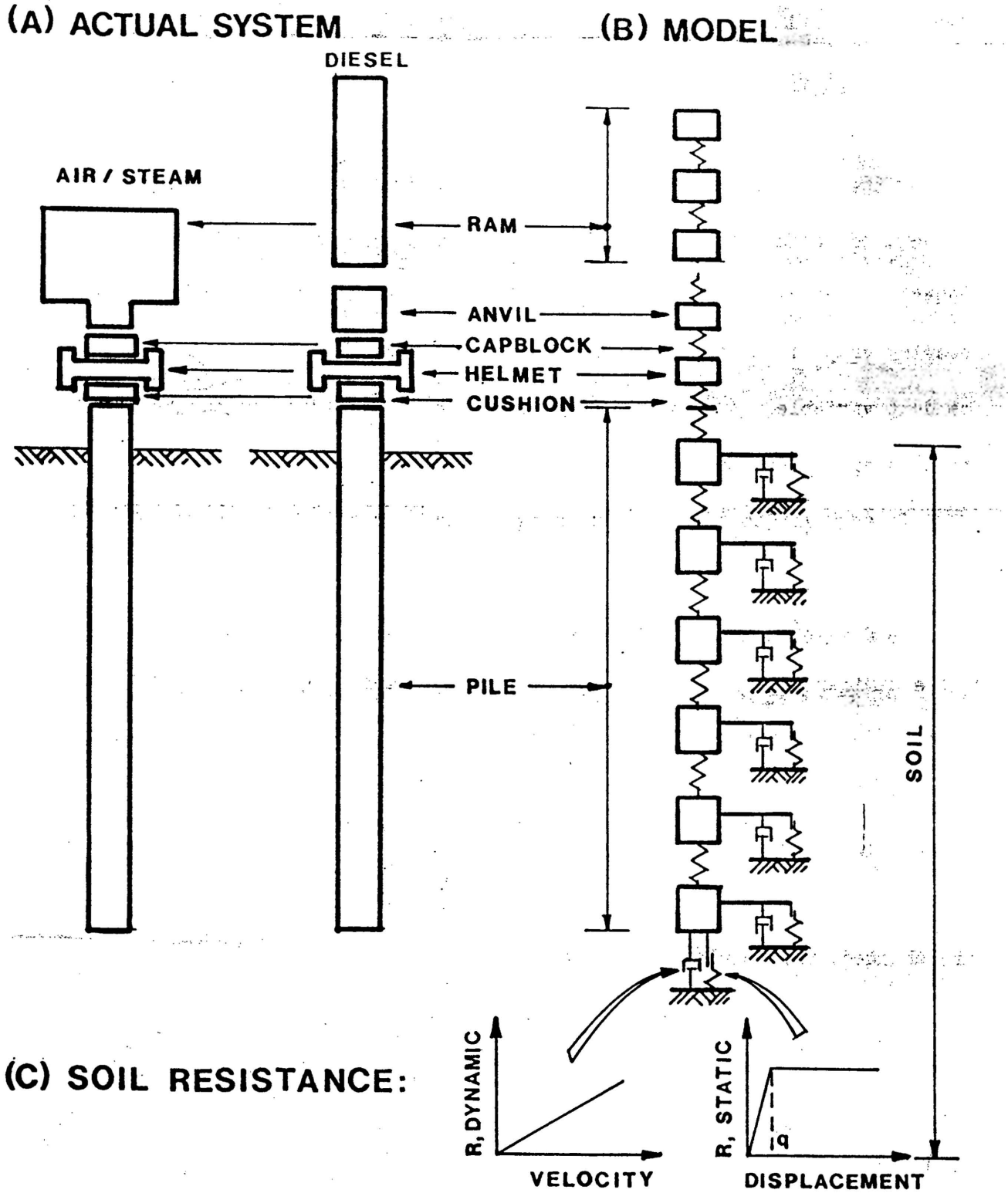

Figure 2. Actual Soil-Pile System and Idealized Schematic Model

The ram, capblock, pile cap, cushion block, and pile are represented by appropriate discrete weights and springs. The frictional resistance on the side of the pile is represented by a series of springs and dashpots, while the point resistance is modelled by a single spring and dashpot.

Soil does not follow the constitutive laws for an isotropic linear-elastic material by being highly nonlinear for large strains and able to deform plastically as well. Smith's model of the constitutive laws of a typical soil subjected to a stress reversal is shown in Fig. 3.

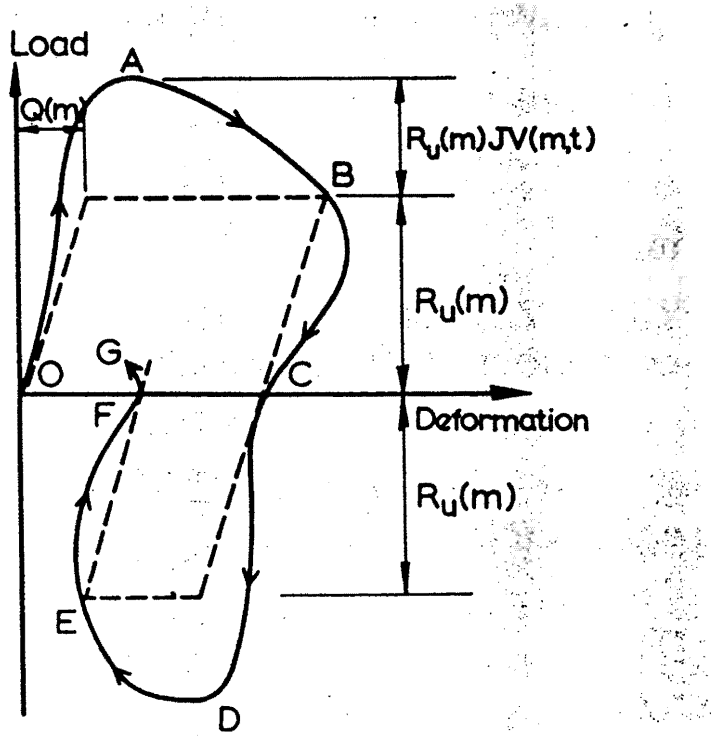

Figure 3. Typical Response for Soil Undergoing a Stress Reversal

The loading path OABCDEFG represents loading and unloading in side friction. For the pile point, only compressive loading is considered and the loading and unloading path in OABCF. The Q(m) term, called the quake, is defined as the maximum "linear" deformation the soil may undergo before the onset of plastic deformation. A idealized load-deformation diagram such as in Figure 4a may now be established seperately for each spring, so that

$$K'(m) = \frac{Ru(m)}{Q(m)}$$

where K'(m) is the spring constant during elastic deformation for the external spring (m). To account for the effects of dynamic loading during pile driving in increasing the instantaneous resistance of the soil, a Kelvin-type rheological model is used (Figure 4b). In the Kelvin model, the damping constant, J, represents the an additional resisting force which is proportional to the velocity of loading.

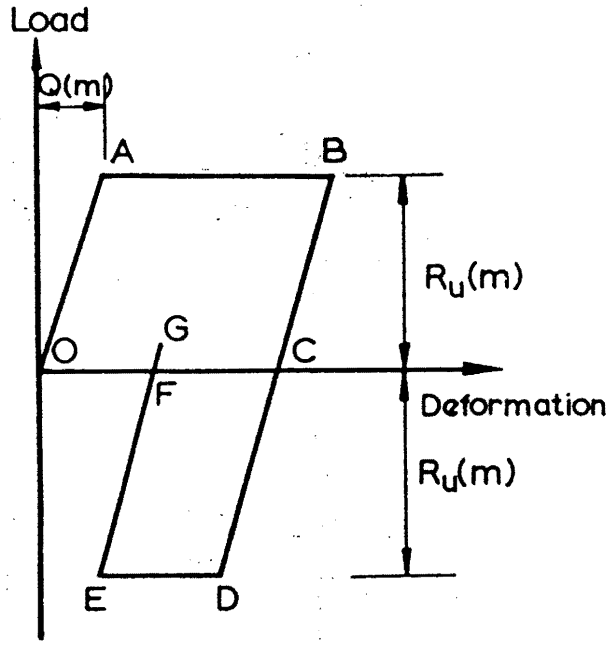

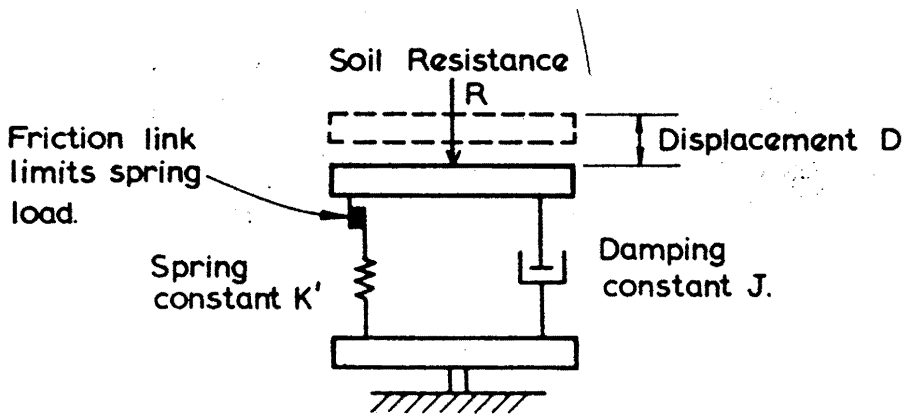

Figure 4. Idealized Elasto-Plastic Stress-Strain Behavior of Soil (a), and Visco-Elastic Model (b)

There is considerable uncertainty regarding the selection of quake and damping values to be used in a WEAP analysis. However; a

commercially available electronic pile driving analyzer, using a sampling probe attached to the pile butt during driving, can monitor and determine in-situ quake and damping values. These values together with a computer program, called CAPWAP[4], further refines WEAP prediction accuracy.

The WEAP-86 Program

In order to model and predict pile load capacity using WEAP-86, the soil and pile physical properties must be input to the computer program via a data input program called W86-IN. Required physical properties include pile driving hammer information, pile and helmet cushion weights, lengths, and stiffnesses, pile-segment discretization properties including masses, damping, and stiffnesses; and soil-pile damping and soil quake values. The WEAP program provides default values for the soil input parameters for toe and side quake terms (.1 in.) and toe and side damping terms (.1 sec./ft.).

The material properties required by the WEAP-86 finite-difference code include the modulus of elasticity of the pile helmet, pile segments, and pile cushion. In addition, assumed skin-friction distribution schemes and end-bearing/skin friction percentages, soil quake values, and damping values all must be specified. A sample input card is shown in Figure 6 which describes the soil-pile system of Figure 1.

```
type v.out
1                    ECHO PRINT OF INPUT DATA

 hpile pg 75 I
  0   0 206   0   0   0   6   0   0   0  15   0   6   0   0   0   0   0
  1.200      .000       .0       .000       .800       .010       .0
   .000       .0       .000       .500       .010       .0
 30.500    21.760 30000.000   492.000       .850       .010
VULCAN  VUL   06   3   1   0
 6.5000   39.1900   17.4900    3.0000    3.0000      .6700
   .000      .000      .800      .010    2
 2.350     2.350      .000   21709.8   21709.8        .0
 .0000     .0000     .0000     .0000     .0000
 .100      .100      .100      .100
     100.0     150.0     250.0     350.0        .0        .0        .0
       .0        .0        .0
1     WEAP86: WAVE EQUATION ANALYSIS OF PILE FOUNDATIONS
                1986, VERSION 1.001

          hpile pg 75 I

           HAMMER MODEL OF: VUL   06 MADE BY: VULCAN

      ELEMENT      WEIGHT  STIFFNESS  COEFF. OF    D-NL.    CAP DAMPG
                   (KIPS)   (K/IN)   RESTITUTION    FT      (K/FT/S)
             1     6.500
      CAP/RAM      1.200  177783.5      .800      .0100       26.3

      ASSEMBLY     WEIGHT STIFFNESS   COEFF. OF   D-NL.
                   (KIPS)   (K/IN)   RESTITUTION   FT
             1     2.350   21709.8
             2     2.350   21709.8       .800      .0100

      HAMMER OPTIONS:
       HAMMER NO. FUEL SETTG. STROKE OPT. HAMMER TYPE DAMPNG-HAMR
         206           1           0           3           2

      HAMMER PERFORMANCE DATA
       RAM WEIGHT  RAM LENGTH   MAX STROKE     STROKE   EFFICIENCY
         (KIPS)       (IN)        (FT)         (FT)
            6.50       39.19       3.00         3.00        .670

       RTD PRESS.   ACT PRESS.   EFF. AREA  IMPACT VEL.
         (PSI)        (PSI)       (IN2)      (FT/S)
             .00          .00         .00       11.37
1
           WEAP  OF  1986              hpile pg 75 I

      PILE PROFILE:
          LBT    AREA    E-MOD     SP.W.     WAVE SP     EA/C
          (FT)   (IN2)    (KSI)   (LB/FT3)    (FT/S)   (K/FT/S)

          .00    21.8   30000.   492.000   16806.8      38.8
        30.50    21.8   30000.   492.000   16806.8      38.8

                WAVE TRAVEL TIME = 2L/C = =   3.629 MS

              PILE AND SOIL MODEL FOR RULT =     100.0 KIPS

  NO  WEIGHT   STIFFN   D-NL SPLICE     COR  SOIL-S SOIL-D  QUAKE   L BT    AREA
      (KIPS)   (K/IN)   (FT)  (FT)          (KIPS) (S/FT)   (IN)    (FT)  (IN**2)
   1    .378   10702.   .010   .000   .850    2.5   .100    .100    5.08    21.8
   2    .378   10702.   .010 -1.000  1.000    2.5   .100    .100   10.17    21.8
   4    .378   10702.   .010 -1.000  1.000    2.5   .100    .100   20.33    21.8
   6    .378   10702.   .010 -1.000  1.000    2.5   .100    .100   30.50    21.8
 TOE                                        85.0   .100    .100

      PILE OPTIONS:
      N/UNIFORM  AUTO S.G.  SPLICES  DAMPNG-P   D-P VALUE
                                                 (K/FT/S)
           0          0         0         1        .777

      SOIL OPTIONS:
       % SKIN FR  % END BG   DIS. NO.  S DAMPING
          15         85         6       SMITH-1

      ANALYSIS/OUTPUT OPTIONS:
      ITERATNS  DTCR/DT(%)  RES STRESS   IOUT  AUTO SGMNT OUTPT INCR  MAX T(MS)
          0         160         0         0         0         3         0
```

Figure 5. WEAP-86 Input Card for Pile Installation in Figure 1.

Of considerable interest to the geotechnical engineer are the quake and damping values. These are very difficult to estimate from available soil properties, but experience over the years suggest certain guidelines. Forehand and Reese[5] have compiled some empirical quake and damping values as shown in Table 1. Unless otherwise stated, WEAP-86 provides a default value of .1 in. for toe and side quakes (Smith), and .1 sec./ft. for toe and side damping. These values are the recommended default values for using WEAP-86, unless values from any other rational basis, such as the CAPWAP/dynamic pile analyzer, are available.

Table 1. Empirical Values of QT, DT, and Percent Side Friction[5]

Soil	Q (in.)	$J(p)$ (sec/ft)	Side Adhesion (% of R_u)
Coarse sand	0.10	0.15	35
Sand gravel mixed	0.10	0.15	75–100
Fine sand	0.15	0.15	100
Sand and clay or loam, at least 50% of pile in sand	0.20	0.20	25
Silt and fine sand underlain by hard strata	0.20	0.20	40
Sand and gravel underlain by hard strata	0.15	0.15	25

Failure Criterion

The terms "ultimate load" and "failure" for a pile require some discussion. As stated by Peck[6] et. al., the ultimate or failure load for a friction pile may be constructed graphically simply by extending the two lines obtained from the load vs. settlement curve. For a friction pile these two lines are well-defined. However, for piles that develop significant end-bearing resistance, the load - settlement curve increases monotonically as the load increases due to the skin friction being mobilized first, then the point resistance. Van der Veen[7] has postulated that the load settlement curve is of the general form $P = Pu(1-e^{bx})$, where x is vertical settlement and b is a constant determined by a least square curve fitting scheme.

Van der Veen's criterion defines the failure load as the load value corresponding to the vertical asymtote of the load vs. butt deformation curve. Van der Veen's criteria are shown schematically in Fig. 6. A least square curve fitting computer routine was developed to find Van der Veen's (VDVM) ultimate load from available load - settlement information. However, VDVM indicates excessively large pile capacities for some data. Theoretically, Pu will occur at an unbounded displacement value using the VDVM criterion.

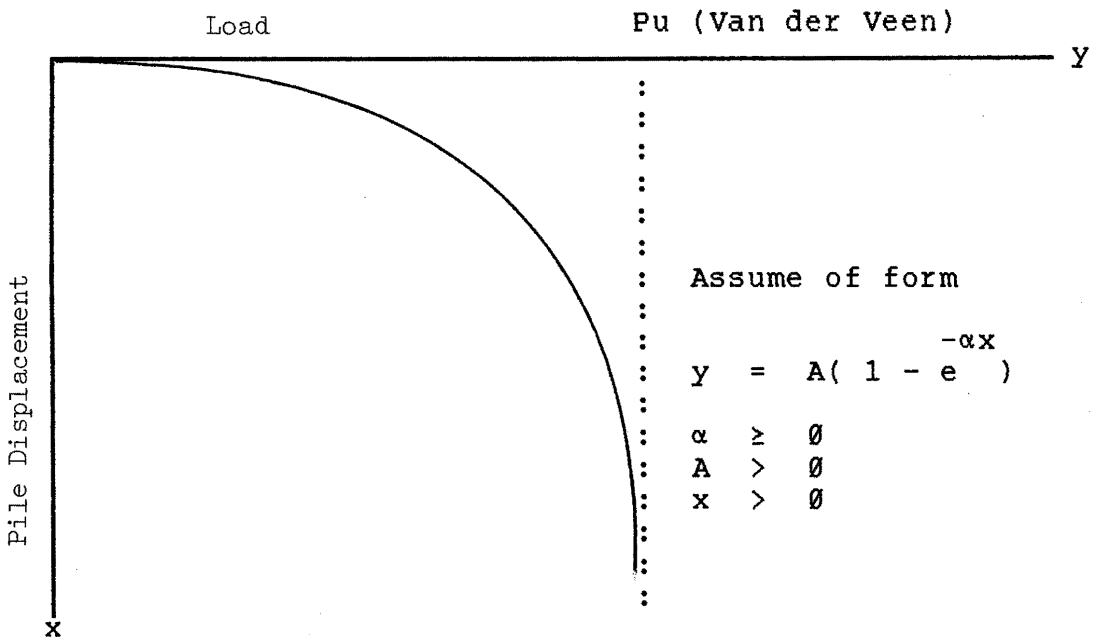

Figure 6. Van der Veen's Approach for Determining Pu.

Alternatively, one could use Terzaghi's criterion[8] which defines P ult. as the load at which pile settlement equals 10% of the pile base diameter. However, this approach fails to consider the load - settlement curve of the pile and the associated soil-pile behavior and may also lead to somewhat high Pu values.

Another unpublished failure criterion, developed by O'Neill[9] plots the time rate change of settlement against applied load. The

generated curve consists of two lines, whose point of intersection corresponds to the failure load as described by O'Neill (Figure 7). In order to use O'Neill's criterion, time vs. settlement curves for each load increment must be available. Since this criterion has only been presented recently, the CONNDOT data base does not contain the necessary information.

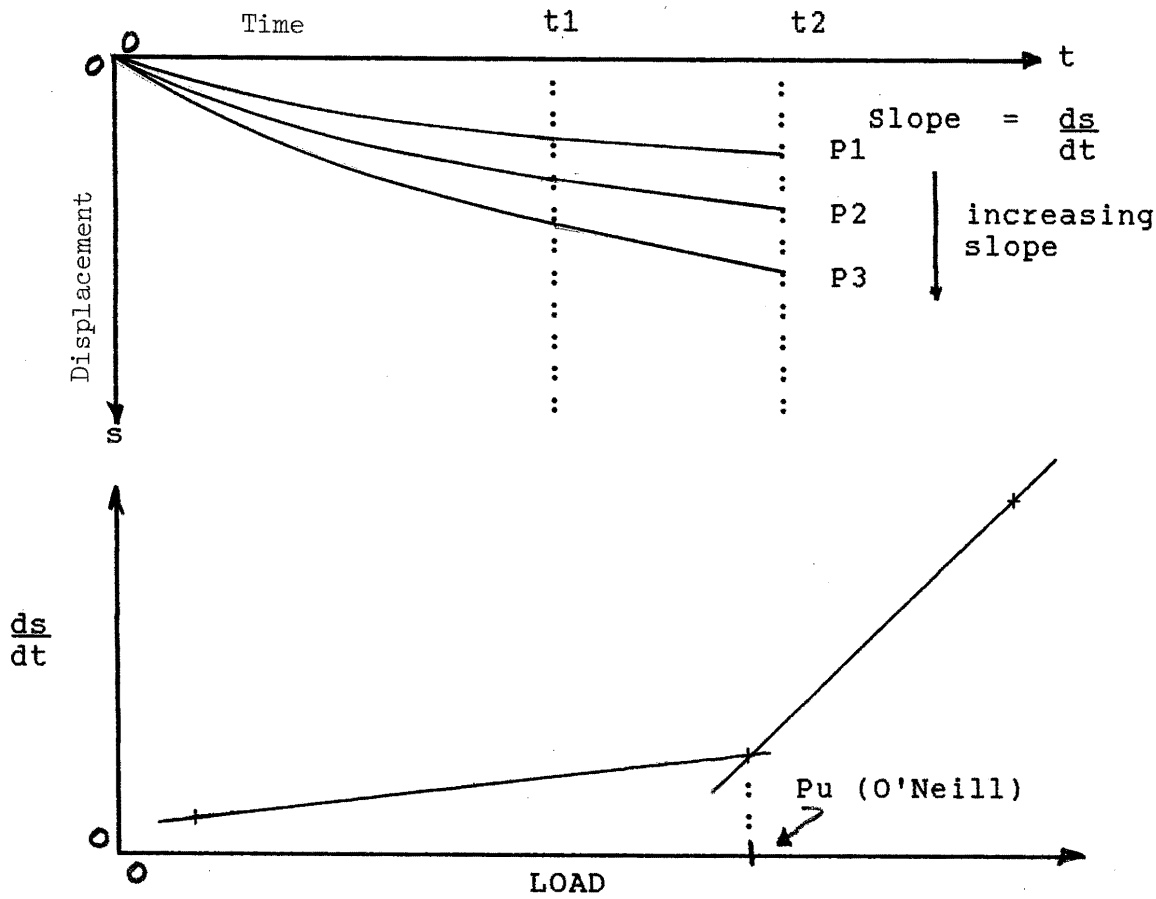

Figure 7. O'Neill's Approach for Determining Pu.

A useful definition for the failure load of a pile could be the point of maximum curvature on the load-settlement curve. This point represents a finite settlement beyond which the settlement per load increment increases. The point of maximum curvature can be determined by eyes.

An example is shown in Figure 8. The degree of curvature is mathematically equal to the 2nd derivative of y with respect to x, and in words represents the rate of change of slope with respect to x. However, for practical purposes, one can locate the point of maximum curvature (minimum radius of curvature) by inspection.

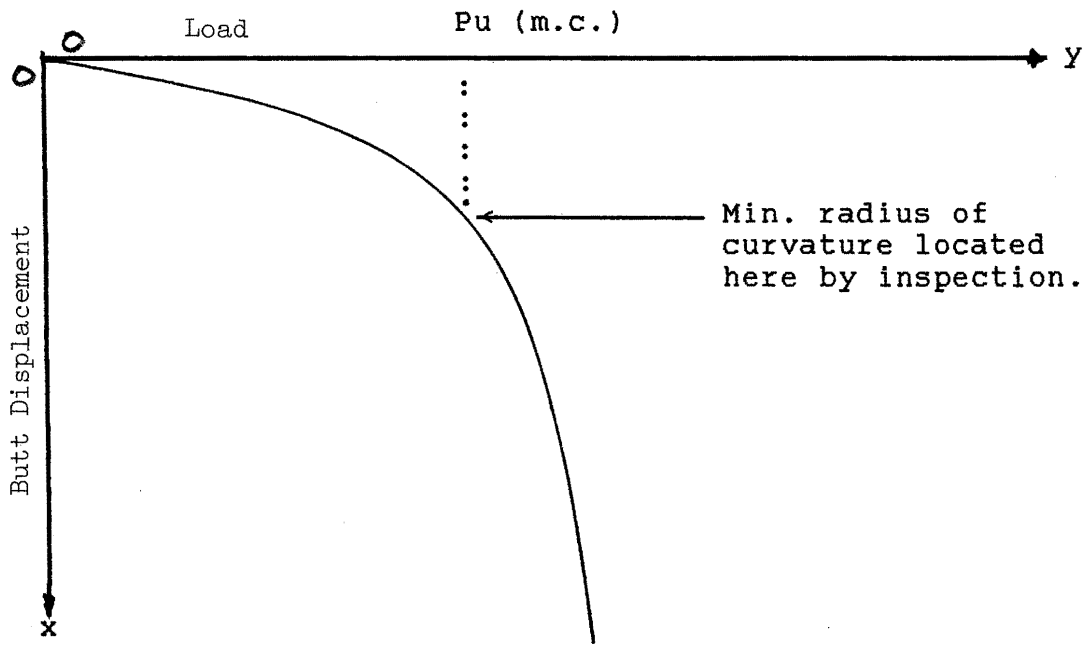

Figure 8. Maximum Curvature Approach for Determining Pu.

The concept of the maximum curvature criterion is along the same lines Peck's criterion for friction piles.

Figure 9 shows a typical load vs. butt settlement curve and a comparison of ultimate capacities obtained from using the VDVM, Terzaghi, and maximum curvature failure criteria.

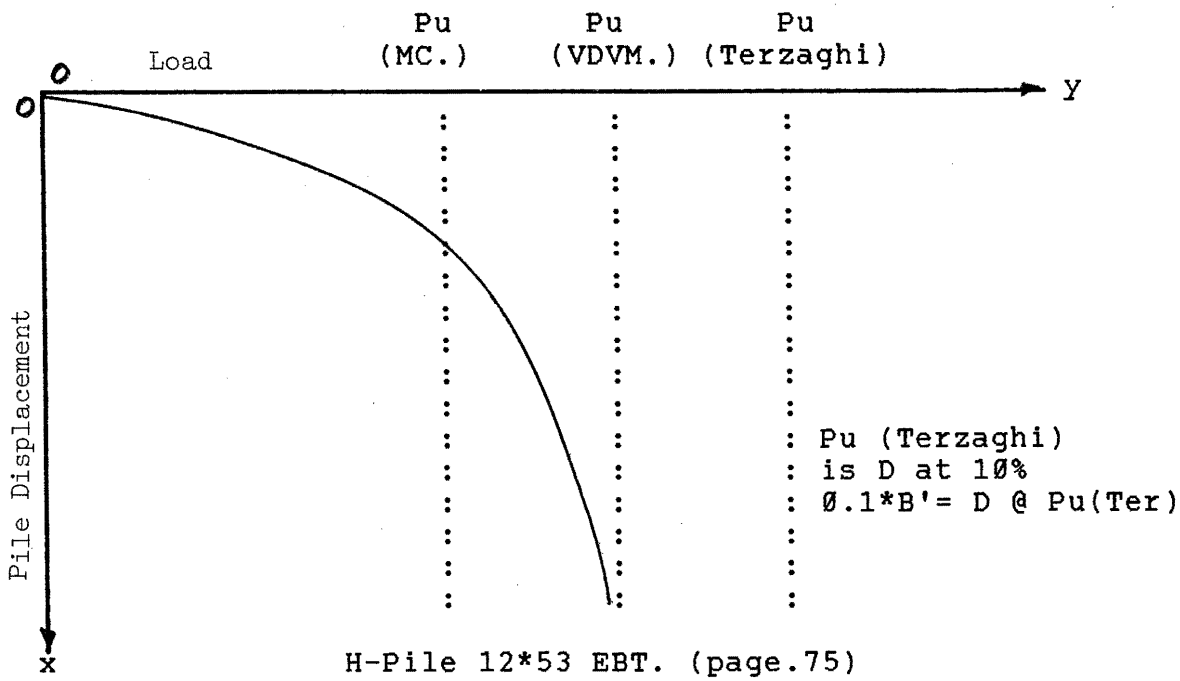

Figure 9. Pu as Obtained by Three Methods

PILE ANALYSIS

The following CONNDOT end-bearing H-pile and friction monotube pile installations were modelled using WEAP-86 and the program default values for quake and damping. Their actual measured capacity from CONNDOT load tests are shown in tabular form in Table 2 as interpreted by two methods: VDVM and maximum curvature.

Table 2. Physical Characteristics of Piles Studied.

Table 2

		Pile Capacity Prediction By				
Location	Pile Size	VDVM.	Max. Curv.	AASHTO.	WEAP.86	Note
I-84 Hartford Pier#4-WB	Steel H 12BP53	352	426	151	210	15% Skin #7 Dist., Smith WT = 0.75
I-84 Hartford, West - Abutment	Steel H 12BP53	282	250	135	450	25% Skin #3 Dist., Smith WT = 0.75
I-84 West Hartford, Pier 1	Steel H 12BP53	318	270	140	305	15% Skin #6 Dist., Smith ST = 0.75
I-84 Hartford,	Steel H 10BP42	278	190	124	180	10% Skin #2 Dist., Smith WT = 0.75
I-84 Hf Over NY.NH. & HRR.	Steel H 12BP74	318	220	131	130	25% Skin #6 Dist., Smith WT = 0.75
I-84 Hartford E.B. Road Way	Steel H 12BP42	356	300	175	405	5% Skin #5 Dist., Smith WT = 0.75
I-84 Hartford,	Steel H 10BP42	280	222	117	140	5% Skin #7 E = 1450 psi. den = 75 pcf

Table 2. (Continued)

Location	Pile Size	Pile Capacity Prediction By VDVM.	Max. Curv.	AASHTO. DESIGNLOAD	WEAP.86	Note
I-84 Hartford, S-E Rdwy. Viaduct	Precast Con. 24" Sq., Type III tip.	502	400	227	275	10% Skin #7 Dist., WT = 1.0
I-84 Nook - FarmSewer	Timber, 12" dia. III tip.	42	18	13	9	60% Skin #7 Dist., E = 1450 psi.
Derby, Rt. 34 Bridge over Naugatuk R.	Concrete Monotube	222	156	-	-	75% Skin #2 Dist. Wt = 0.75
Groton Southington I-95	Concrete Monotube	250	180	125	151	50% Skin, #3 Dist. Wt = 0.75
Coventry	Concrete Monotube	304	264	144	168	75% Skin, #2 Dist. Wt = 0.75
Farmington	Concrete Monotube	162	124	50	133	60% Skin, #7 Dist.
Coventry I-84	Concrete Monotube	212	150	105	178	75% Skin, #2 Dist.
Derby, Rt. 34 Bridge over Naugatuk R.	Concrete Monotube	224	156	-	85	75% Skin, #2 Dist.

It should be reiterated that the two program input parameters with the greated uncertainty are the soil quake terms and the soil damping terms. Other input terms such as the modulus of elasticity of steel, unit weight of steel, length of pile, and to a somewhat lesser extent, the skin friction distribution, hammer energy transferred to the pile, and cushion stiffness are known to a relatively high degree of accuracy.

The major focus of the study deals with the effect of the selected quake and damping terms upon the predicted pile capacity for end-bearing H-pile capacity; in addition, a number of computer modelled monotube piles considered the effect of different skin friction distribution patterns as well as selected quake and damping valve effects. WEAP-86 predictions were generally conducted by varying only a single parameter at a time so that only the effect of that particular parameter is noted.

a) End Bearing H-Piles

A total of 7 steel H-piles driven into sand/glacial till were selected for study based on availability of appropriate load test information for pile tested to failure. The required information includes soil boring information and blow count data taken during driving. Data from the soil borings are used to estimate the fraction of the ultimate load carried in side friction as well as the distribution of stresses along the pile shaft. WEAP program runs were made using the physical properties of the hammer used, the type of pile driven and the bearing soil. This phase of the analysis used the program default values for the quake and damping (Smith type) terms. The results, shown in Table 2 and plotted in Figures 9a and 9b, suggest that the standard default values of quake (QT=.1 in.)

and damping (DT=.1 sec./ft) for end-bearing H-piles statistically underpredict measured pile capacity as interpreted by either the Van der Veen or maximum curvature failure criterion (Figs. 10a and 10b).

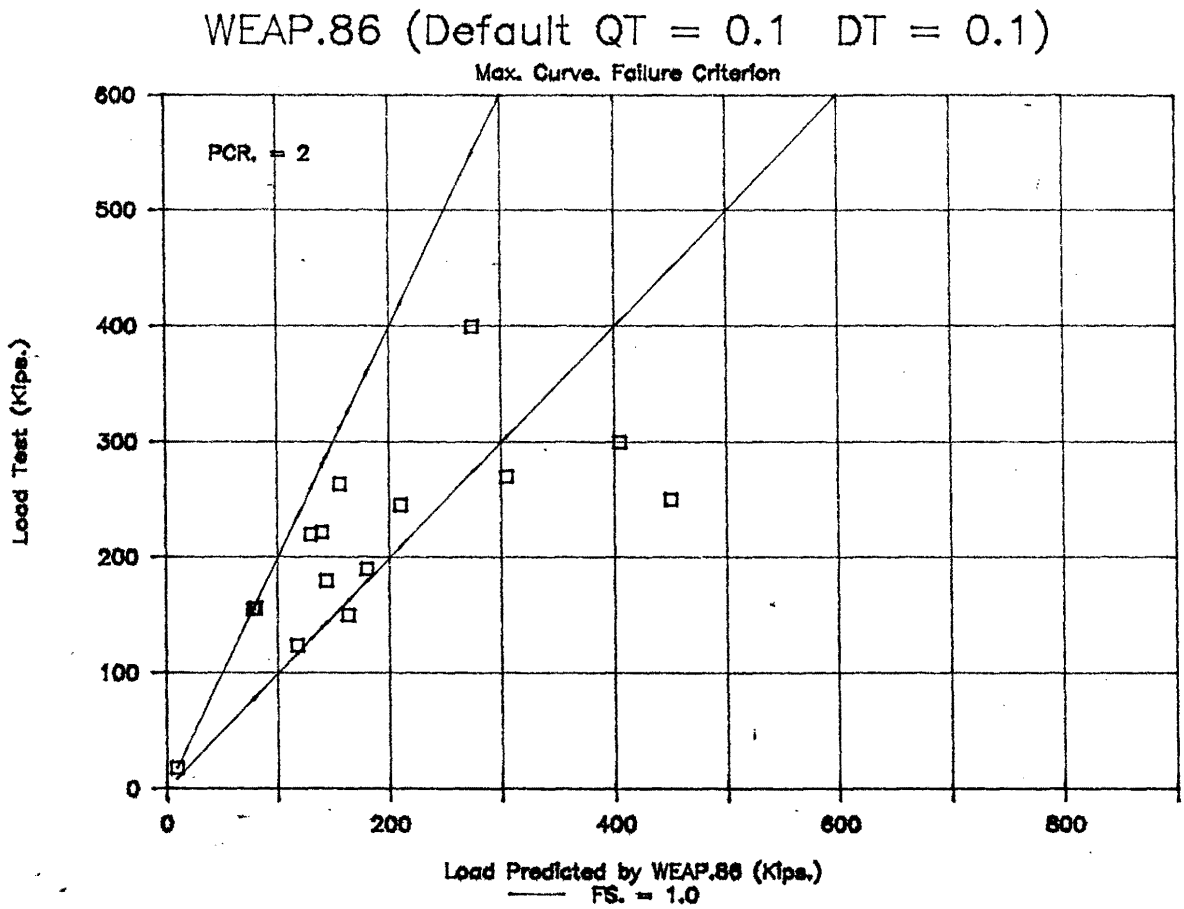

Figure 9a

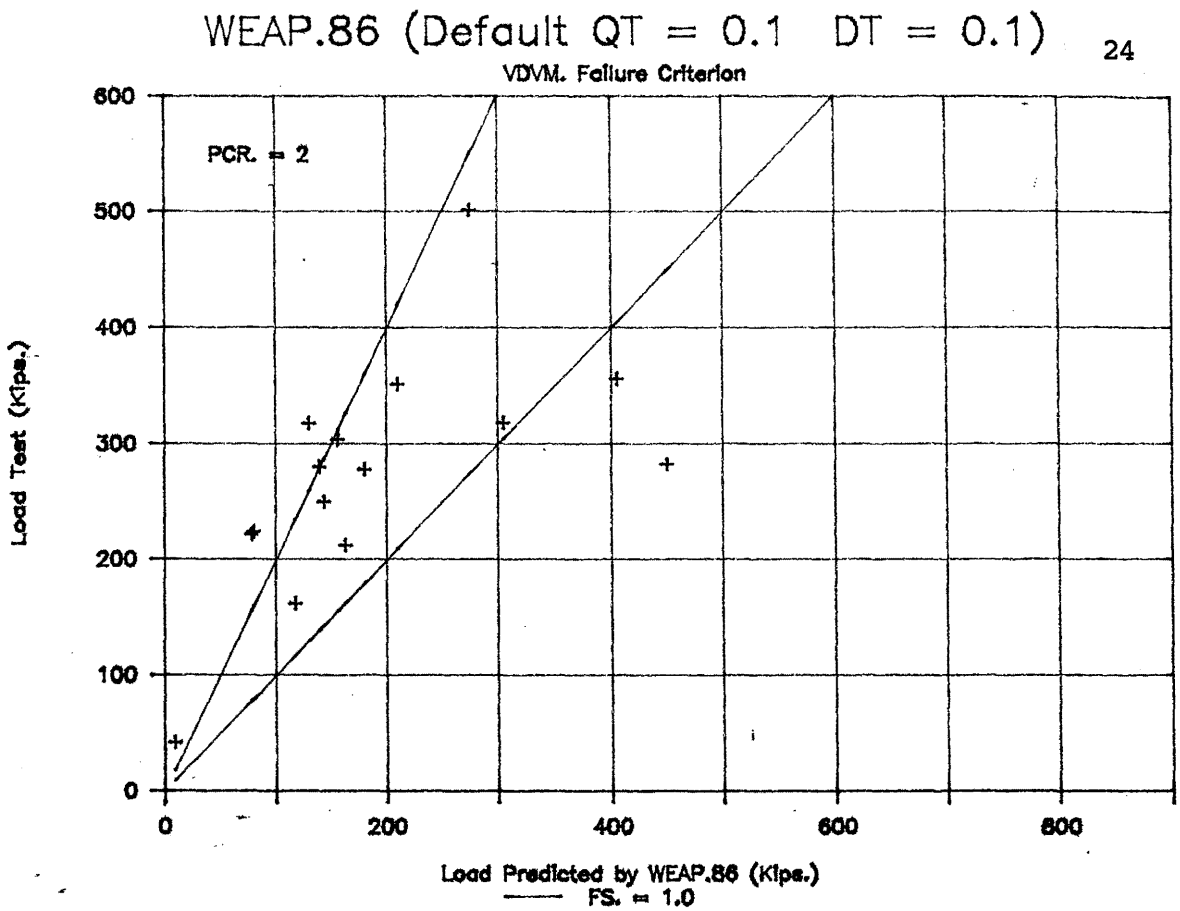

Figure 9b

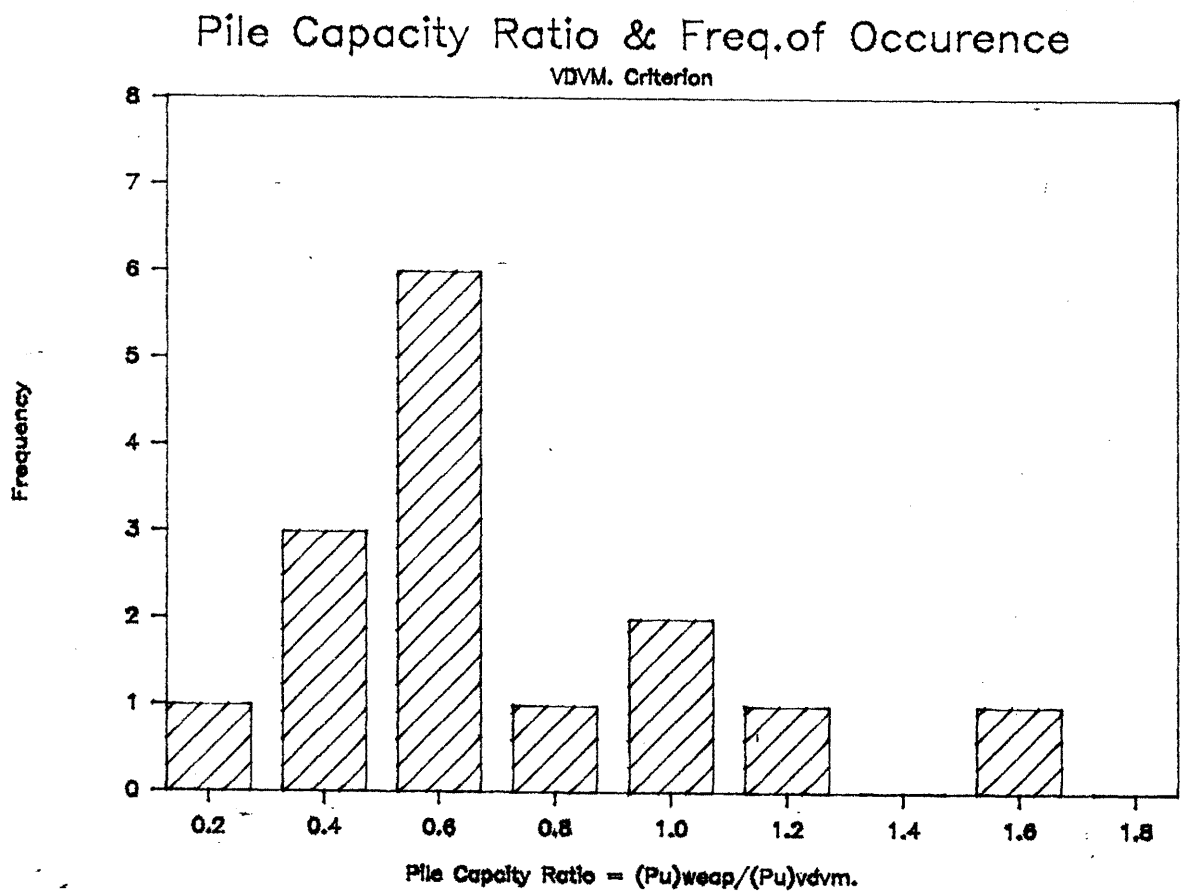

Figure 10a

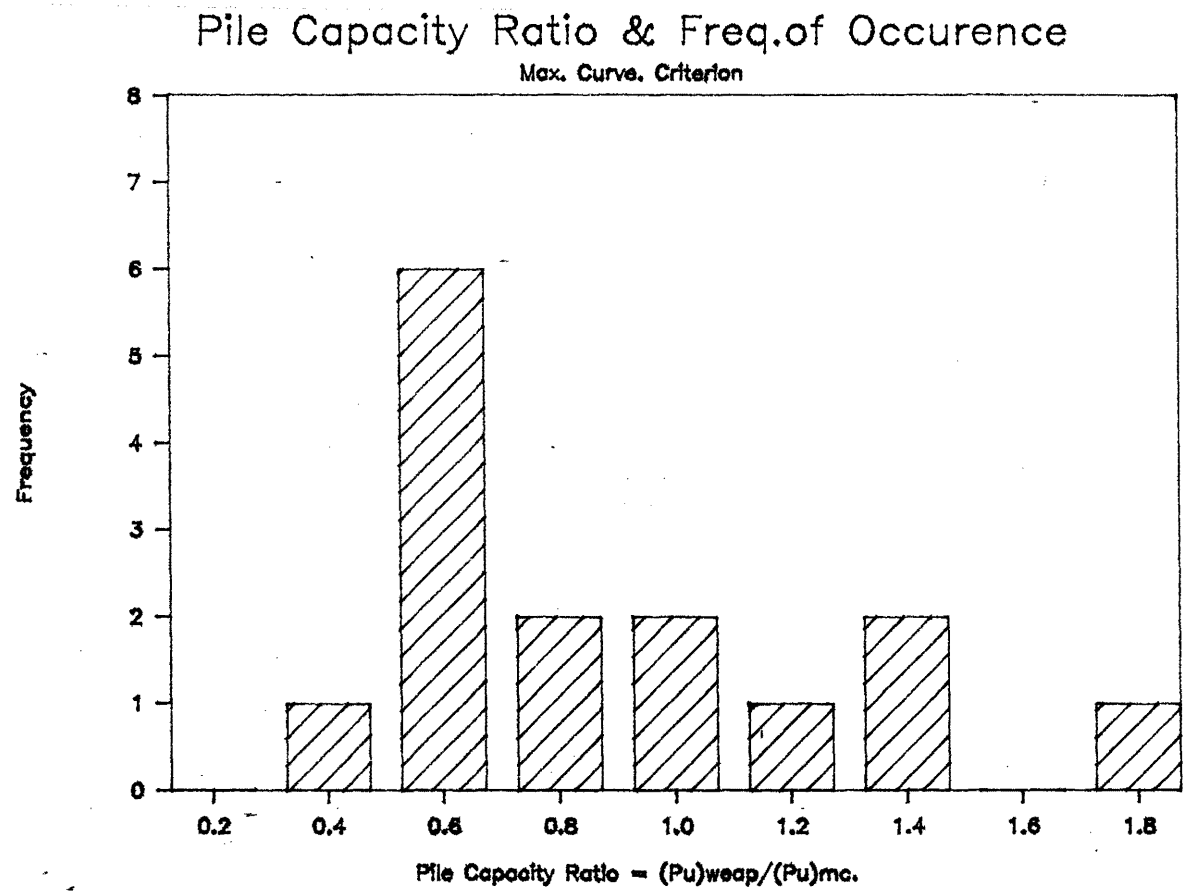

Figure 10b

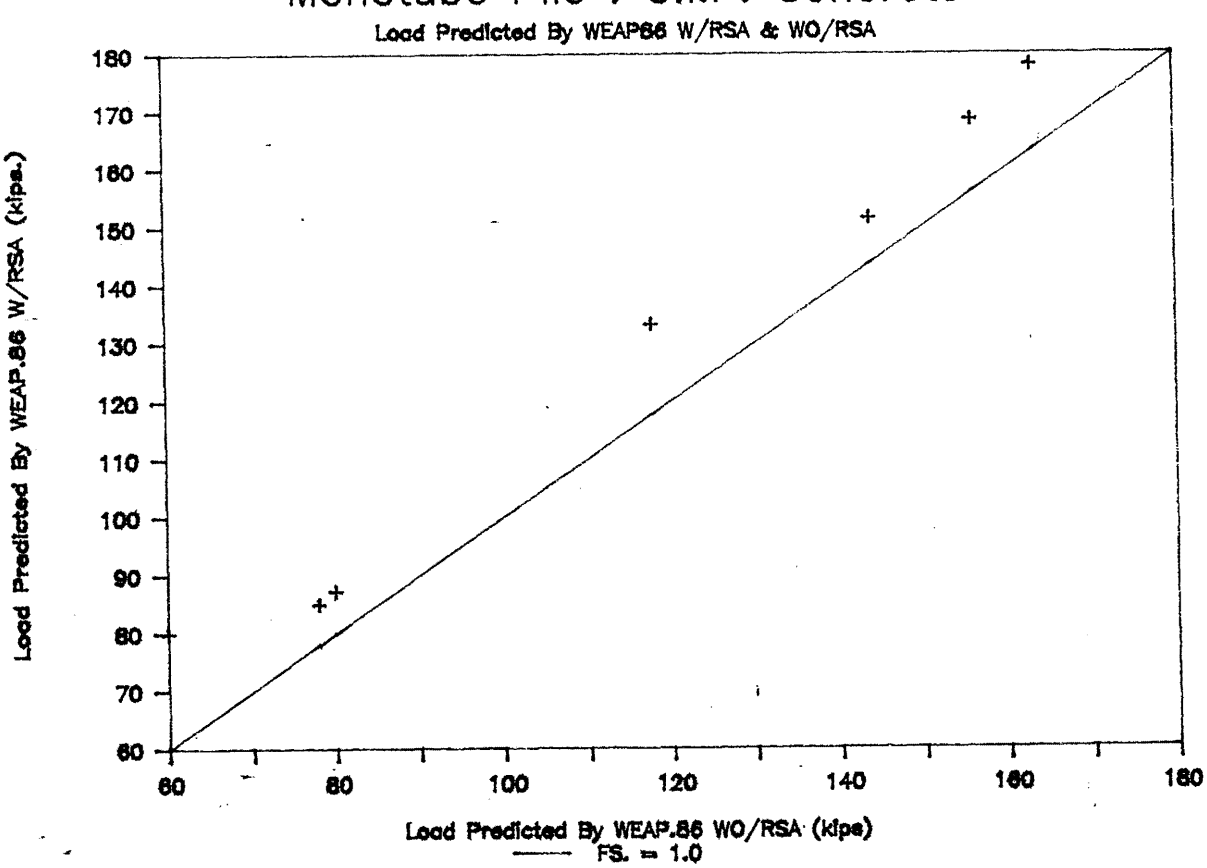

Figure 11

b. Monotube Piles

Seven monotube pipe piles were also modelled using WEAP-86. Monotube piles are normally used as friction piles. The effect of the assumed skin friction distribution along the pile shaft requires consideration as to the residual stresses, damping, and quake values. The importance of residual stresses developed in driven piles has been demonstrated by Holloway[10]. The compression of the pile and soil on the downward stroke when the ram rebounds results in the retention of compressive forces in the lower part of the pile, and these appear to depend on the soil-pile interaction only, independent of the impact driving apparatus used. The magnitude of the residual loads increase as the axial stiffness of the pile decreases. Impact driving of a pile with low axial stiffness will cause the pile to compress in the vertical direction and expand in the radial direction. As the hammer rebounds the pile attempts to return to its orginal length, but the soil along the pile resists this expansion through friction. This soil-pile interaction in the pile results in the development of a residual compressive force at the pile tip which remains even without an applied force at the butt end. When a residual load remains after driving, a portion of the pile's end-bearing capacity has already been mobilized as noted by Braud et al. Conventional pile instrumenation are zeroed at this time, ignoring any residual stresses in load test interpretation. The actual end-bearing capacity of the pile is the measured value plus the residual value. While the effects of residual loads are not measured, failure to account for residual stresses in the WEAP analysis leads to low predicted pile capacities (Fig. 11).

Monotube Piles - Analysis

Seven monotube pipe piles bearing in sand were also modelled using WEAP-86. The results, shown in Figures 10a and 10b, suggest that the standard default values of quake (QT=.01 sec.) and damping (DT=.1 sec./ft) together with use of the R.S.A. for monotube piles statistically underpredict measured pile capacity as interpreted by either the Van der Veen or maximum curvature failure criterion.

Sensitivity Analysis

A parametric sensitivity analysis was conducted to investigate the effects of pile-soil parameter variance on H-pile and monotube predicted capacities.

H-piles- A series of WEAP pile capacity prediction runs were made capacity predicitions were made by varying the toe quake from .1 in. to .05 in. and by varying toe damping from .1 sec./ft. to .05 sec./ft. The variance in a given parameter was conducted while holding the other constant in order to note the effect of varying the parameter of interest only, holding all others at default values for Figs. 13 and 14. Fig. 15 shows the effect of varying QT and DT at the same time. Decreasing either parameter by 50% resulted in an increase in predicted pile capacity of about 15%. Figures 16a. and 16b. show that for QT=0.08 in., for example, the composite actual capacity versus predicted capacity value reflect this increase in predicted capacity by a shift of all points to the right. Other QT and DT values selected (See Figs. 17a, b; 18a, b) show similar trends. A major result from this parameter variation study is that the net accuracy of the solution remains essentially unchanged regardless of QT or DT, provided values near WEAP-86 recommendation are selected. Hence, predicted pile load capacity is not highly

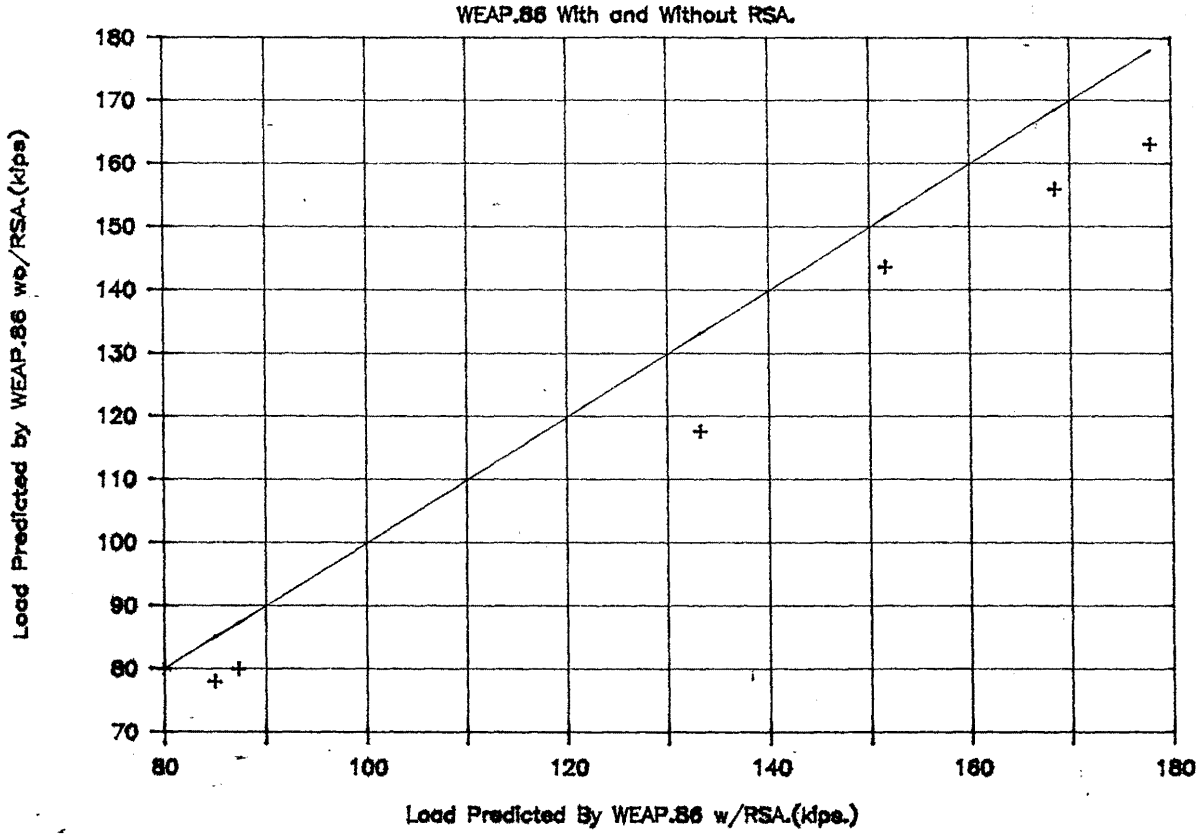

Figure 12

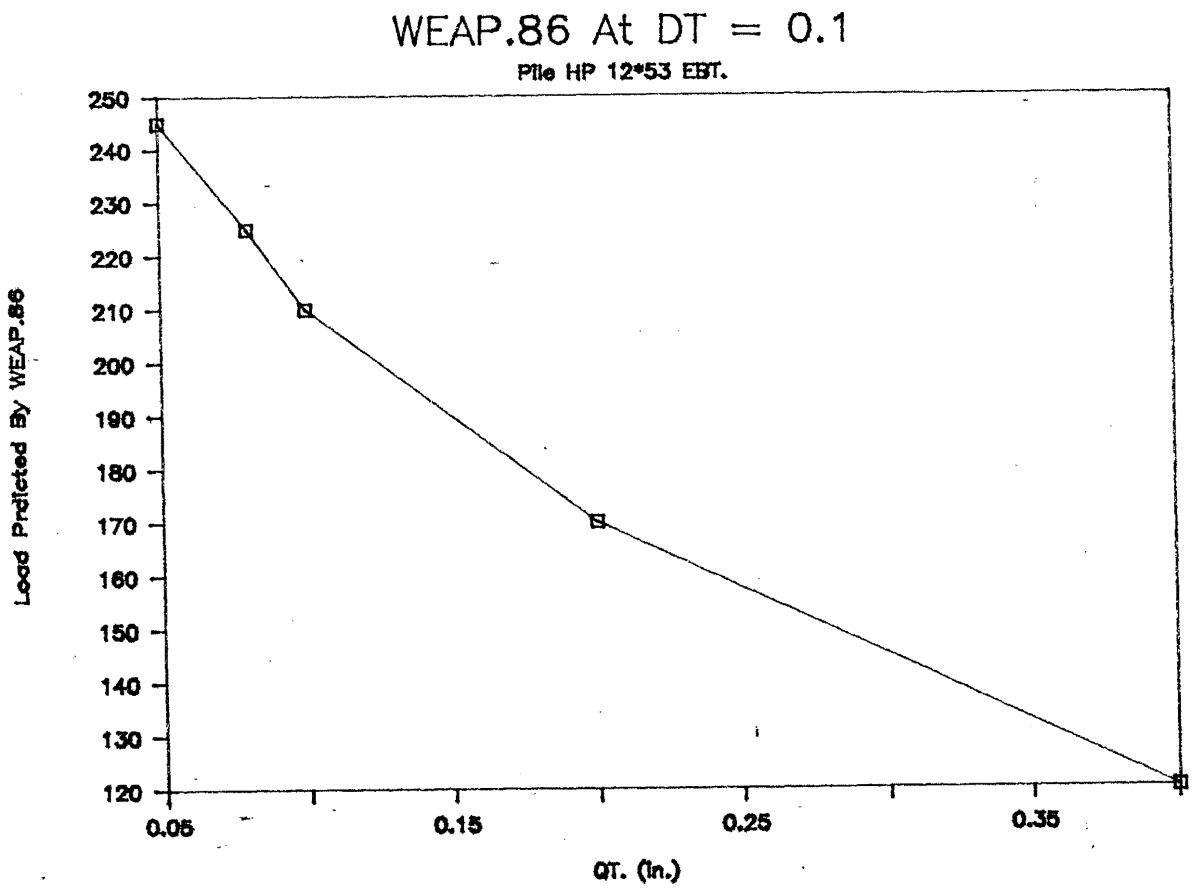

Figure 13

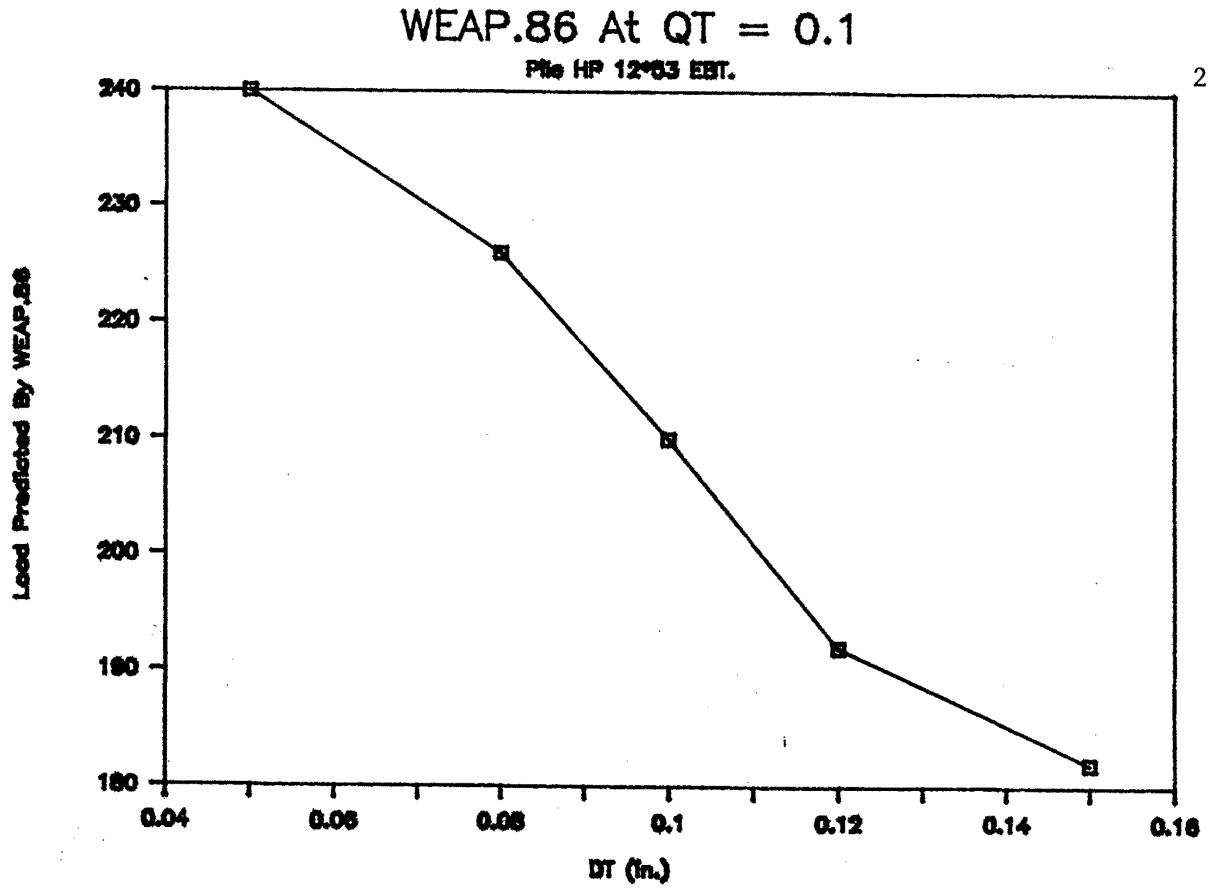

Figure 14

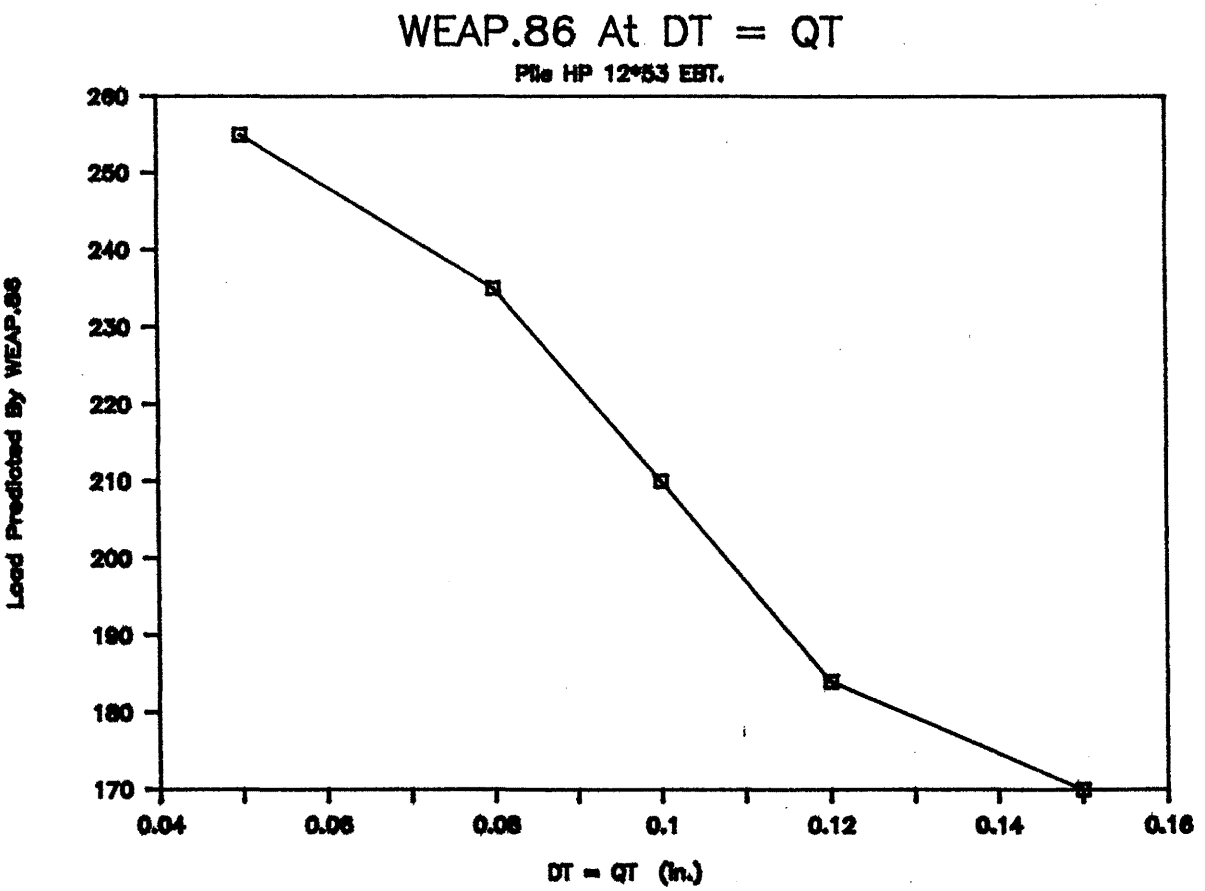

Figure 15

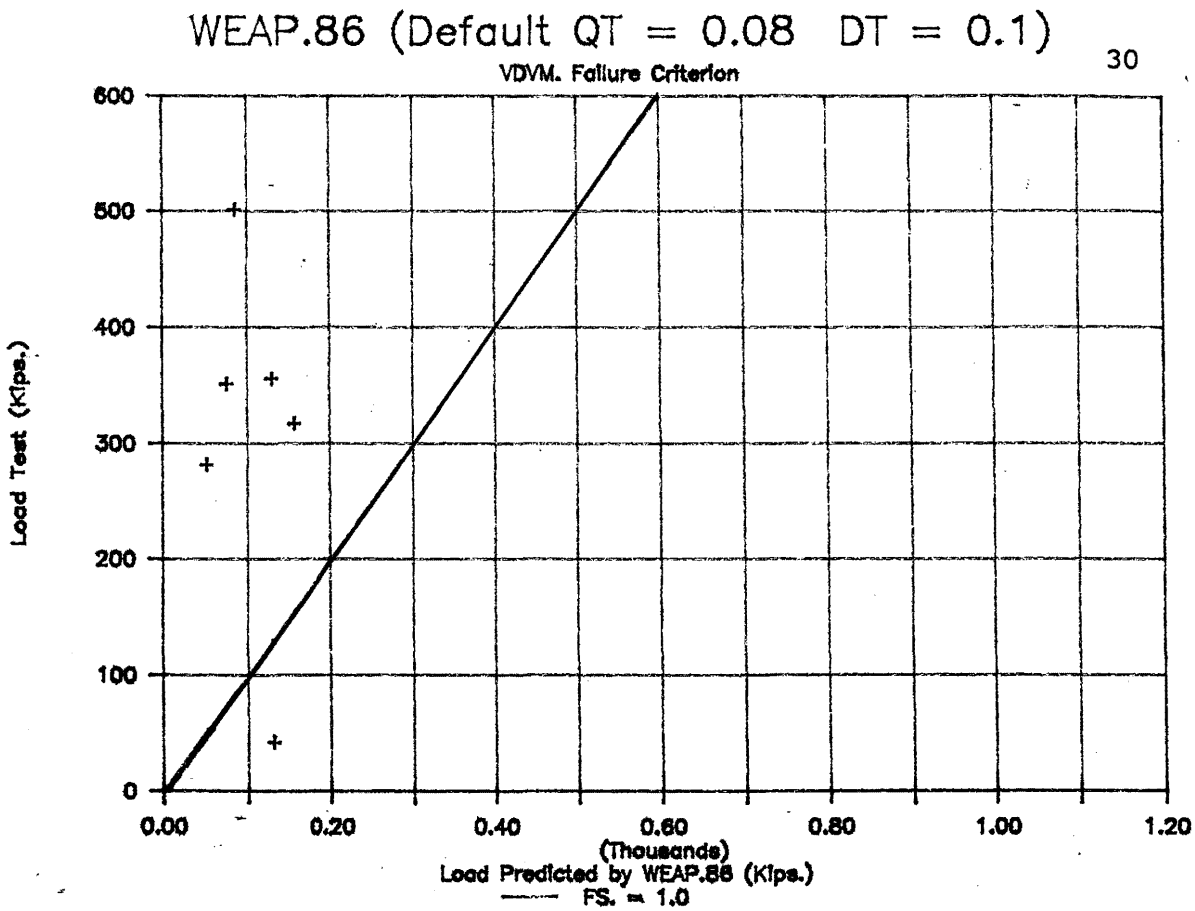

Figure 16a

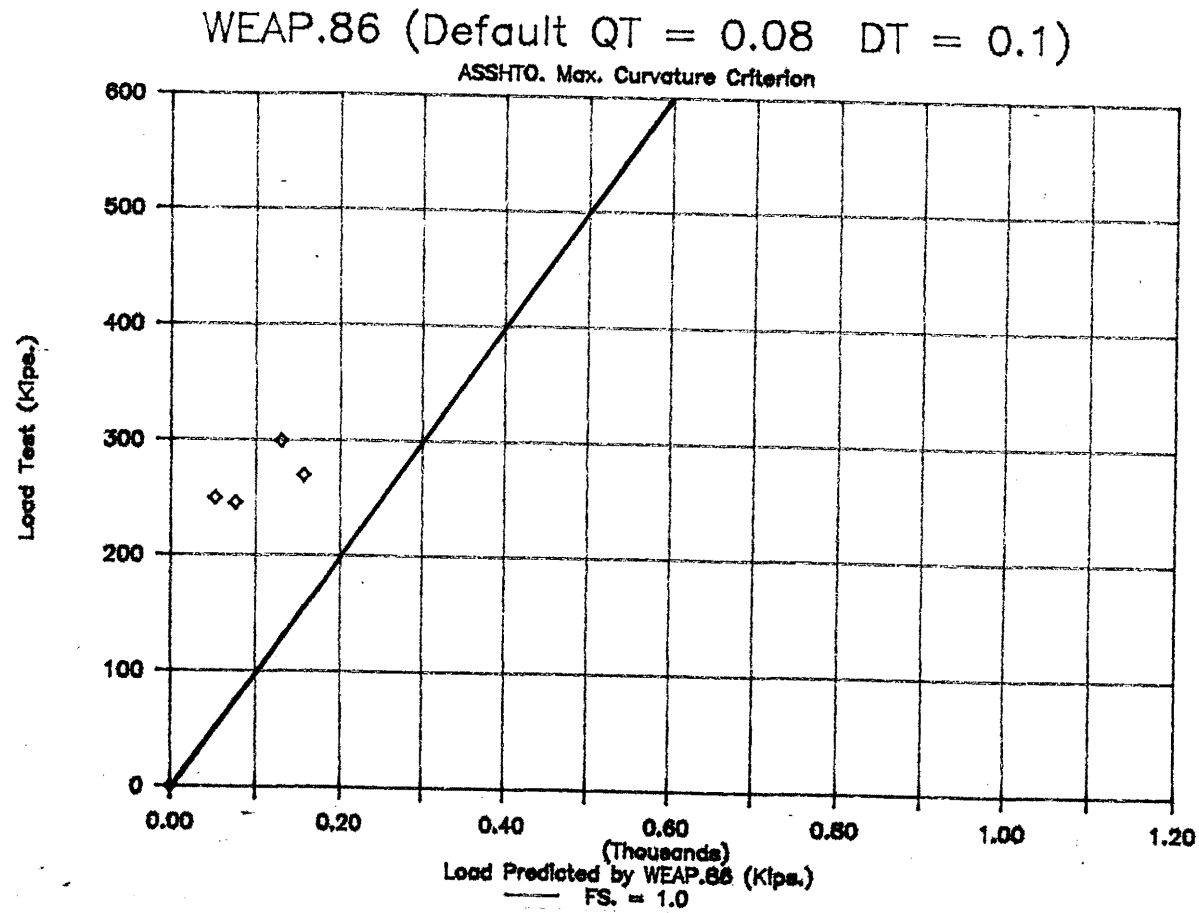

Figure 16b

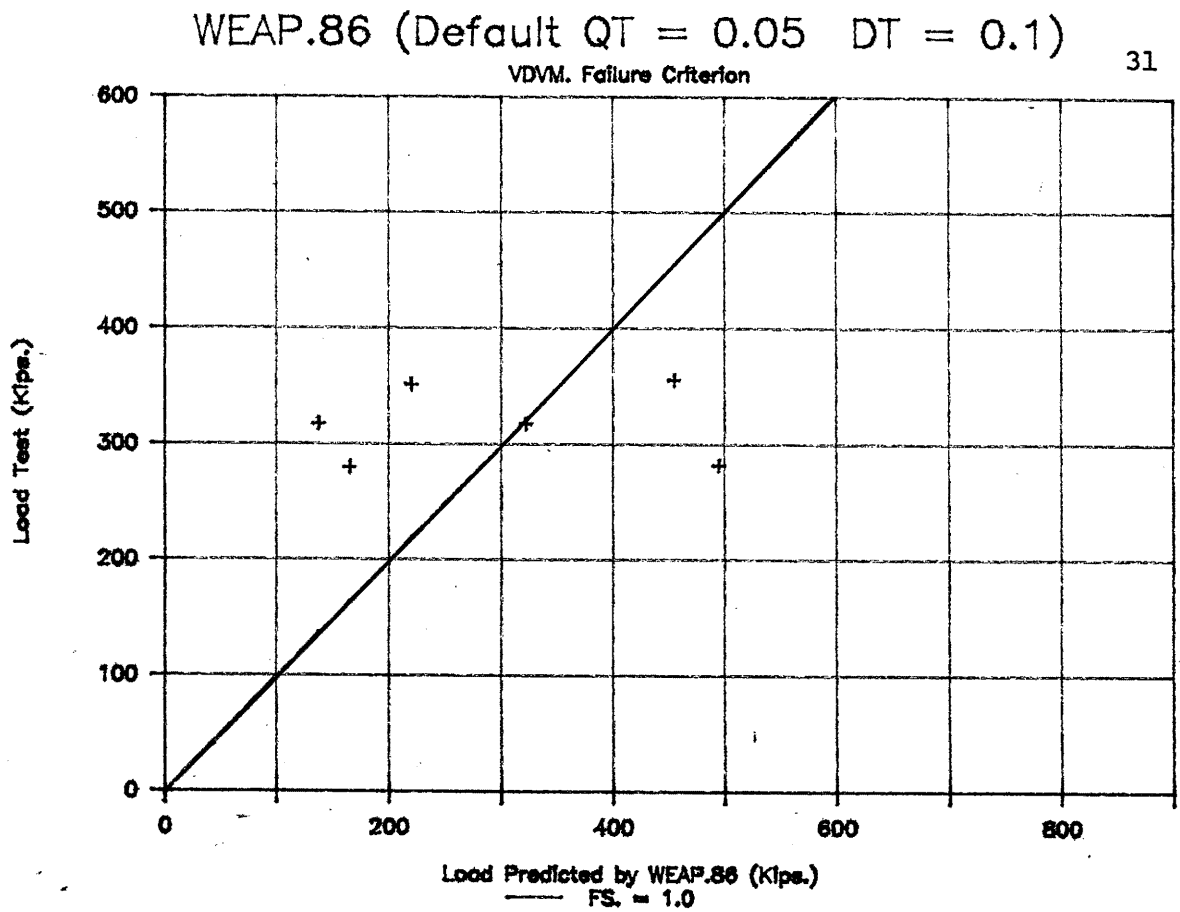

Figure 17a

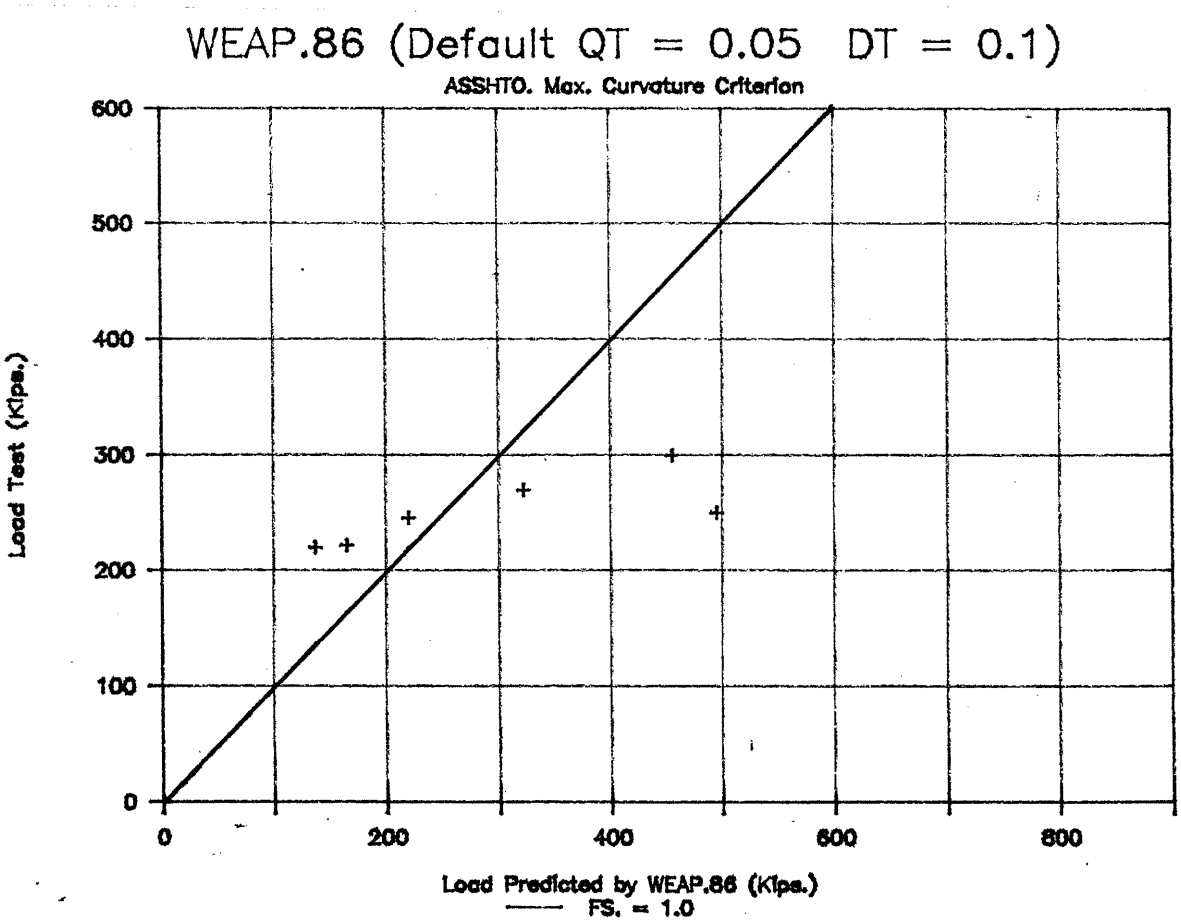

Figure 17b

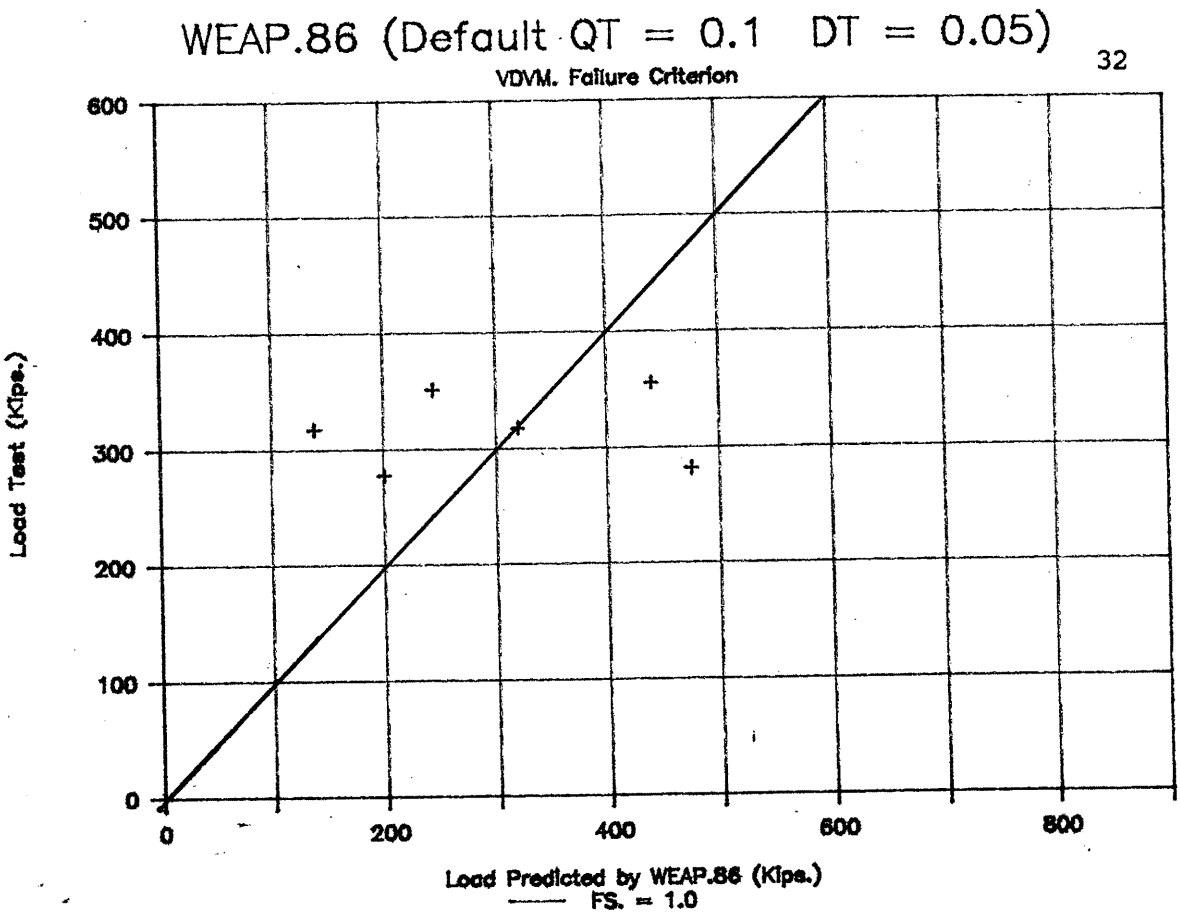

Figure 18a

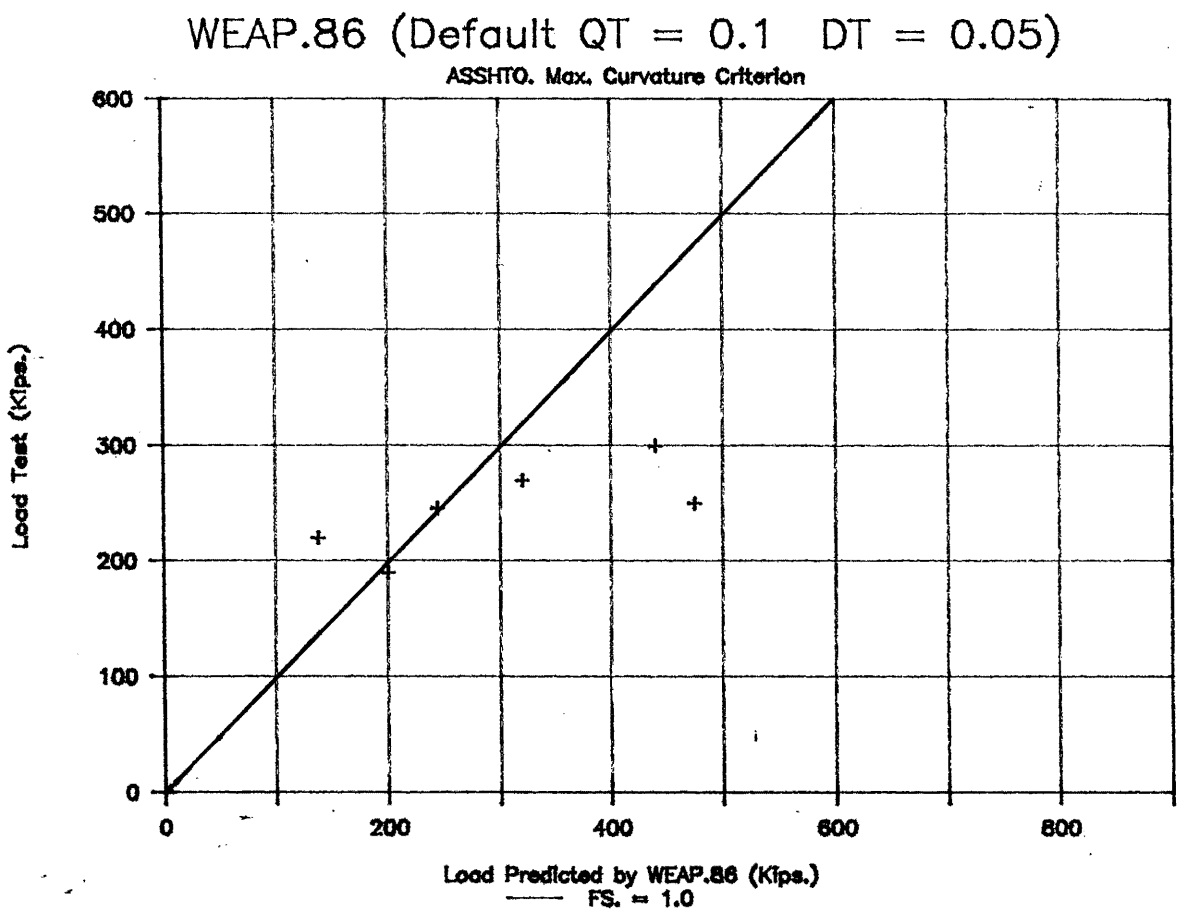

Figure 18b

sensitive to large, +/- 100%, changes in the quake and damping values for end-bearing H-piles.

Monotube piles A series of WEAP pile capacity prediction runs were made by varying the toe quake from .15 in. to .05 in. and by varying toe damping from .15 sec./ft. to .05 sec./ft. Results (Figs 18a,18b) show that a total variation of 15% occurs over the entire range of selected quake and damping values. Next, both parameters were dried to note the composite effect of varying QT and PT at the same time (Fig. 19). Finaly, variation of skin-friction percentage as a fraction of total variation of about 15% occurs from 0% to 100% skin friction assumed of the pile shaft (Fig. 20).

Conclusions

The wave equation analysis of piles (WEAP-86) finite difference computer solution package applied to end-bearing H-piles and friction-type monotube piles in sand show the following trends.

1. Selection of quake and damping values do not appear to greatly influence predicted pile capacity (± 15%).
2. Percent skin friction assumed for monotube piles changes predocted capacity about 15%.
3. Residual Stress Analysis should be used when modelling monotube-type piles.
4. Default values of quake and damping yield predicted capacities that are statistically lower than the measured capacities.
5. WEAP-86 provides the user with some insight into the pile driving process and effects of various properties on the pile stresses and capacities.

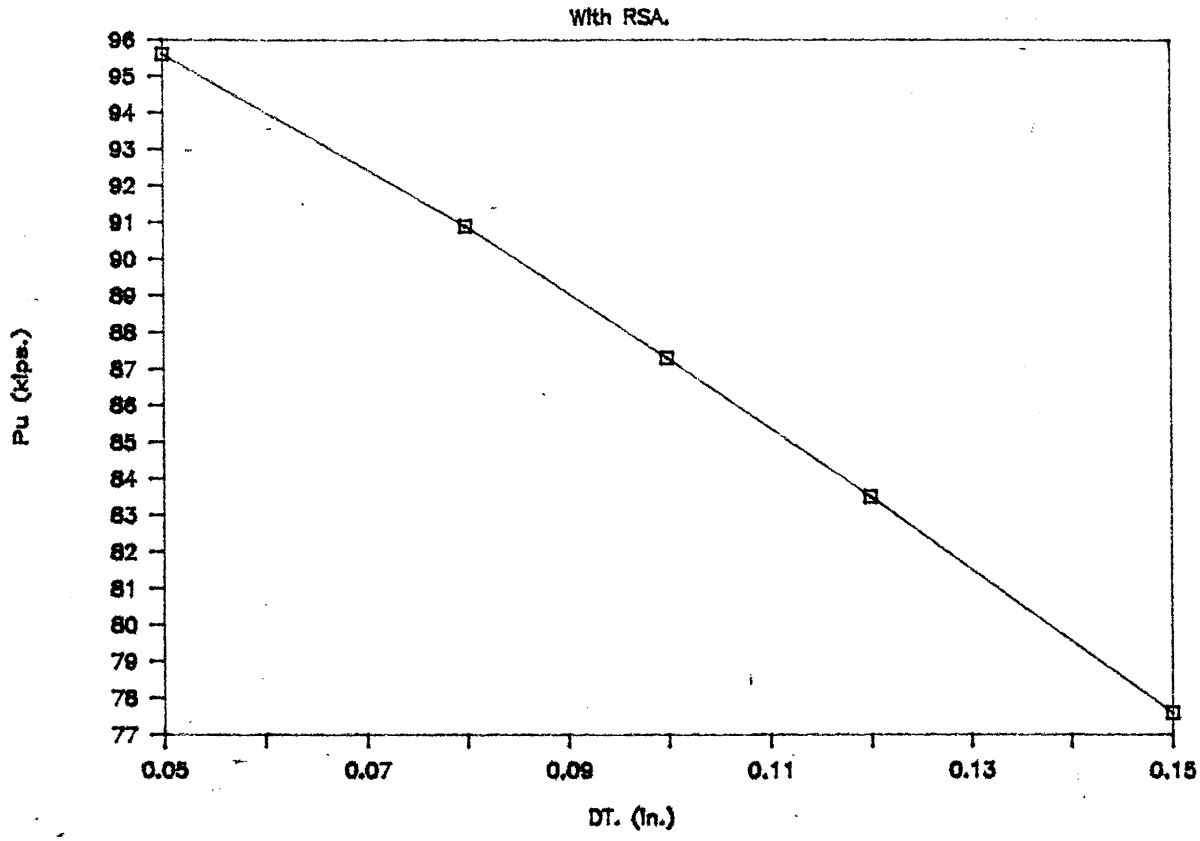

Figure 19a

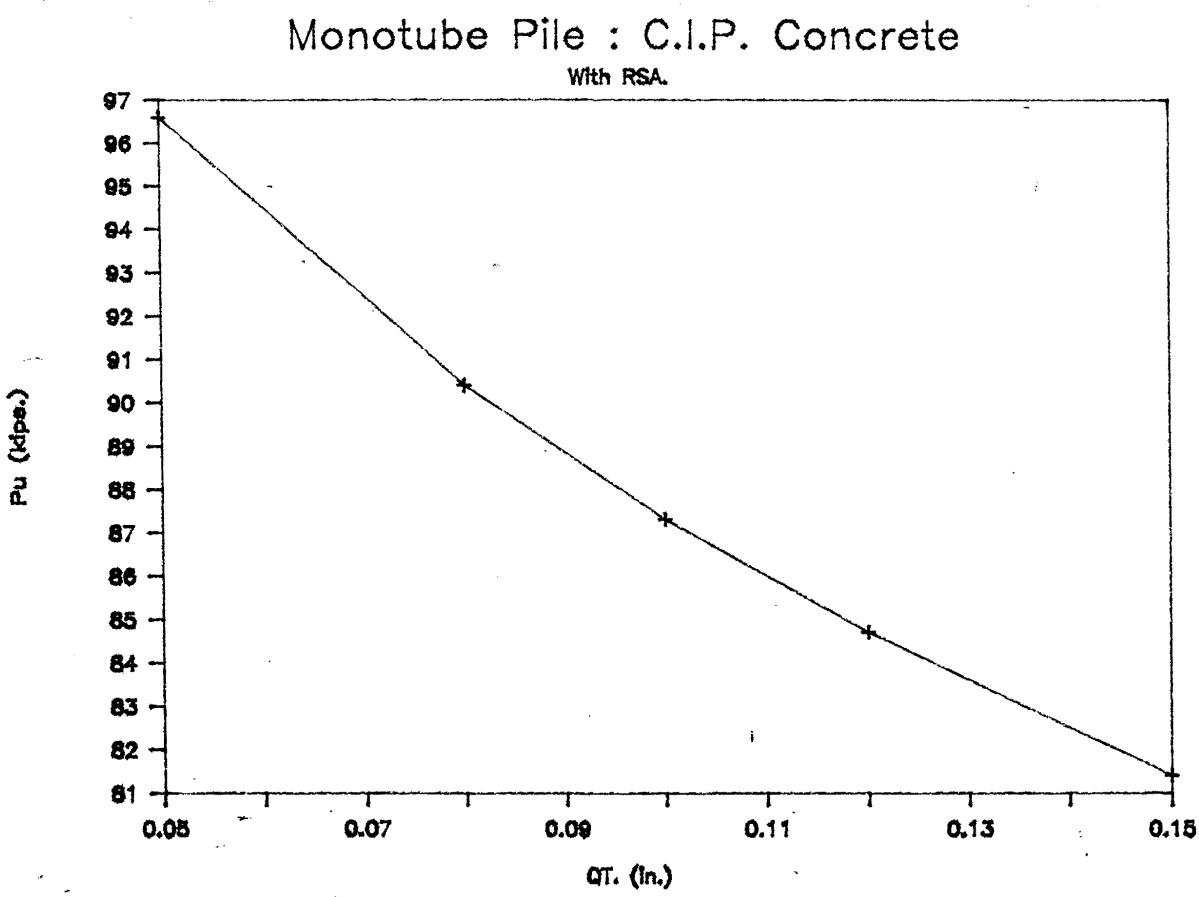

Figure 19b

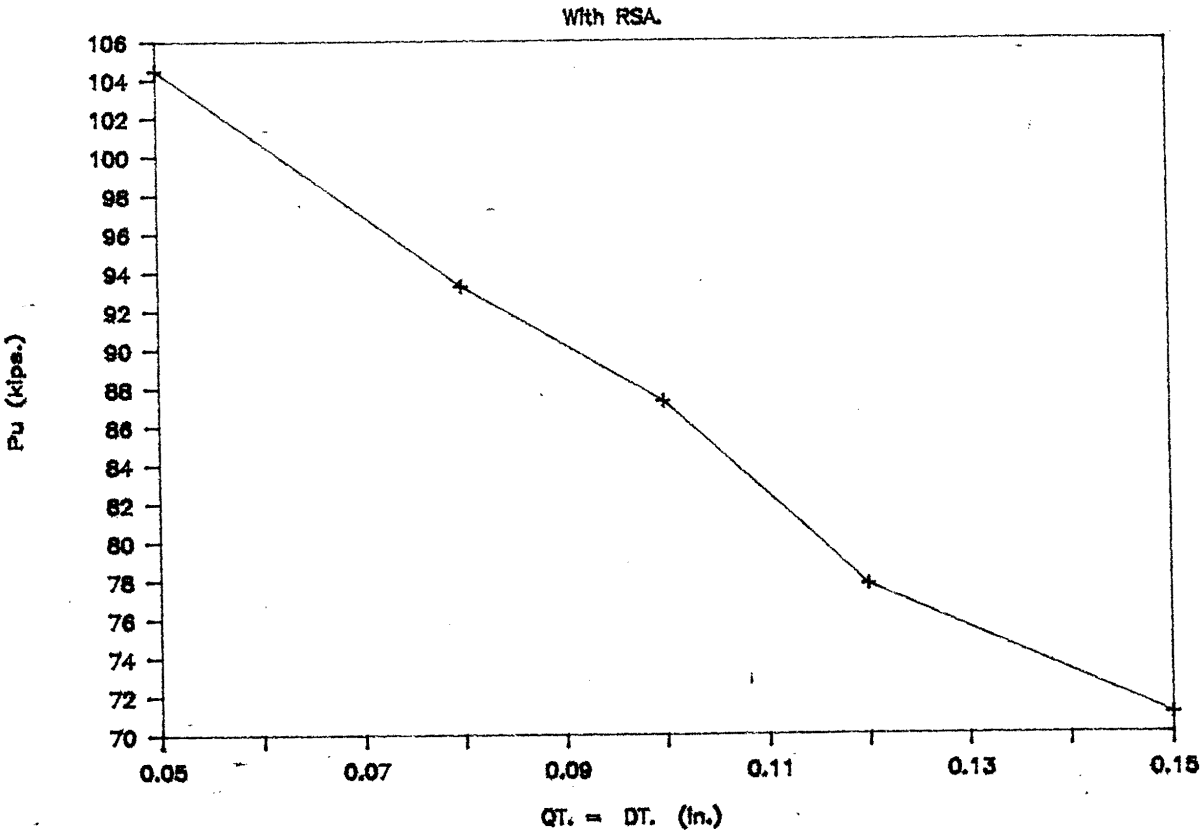

Figure 20

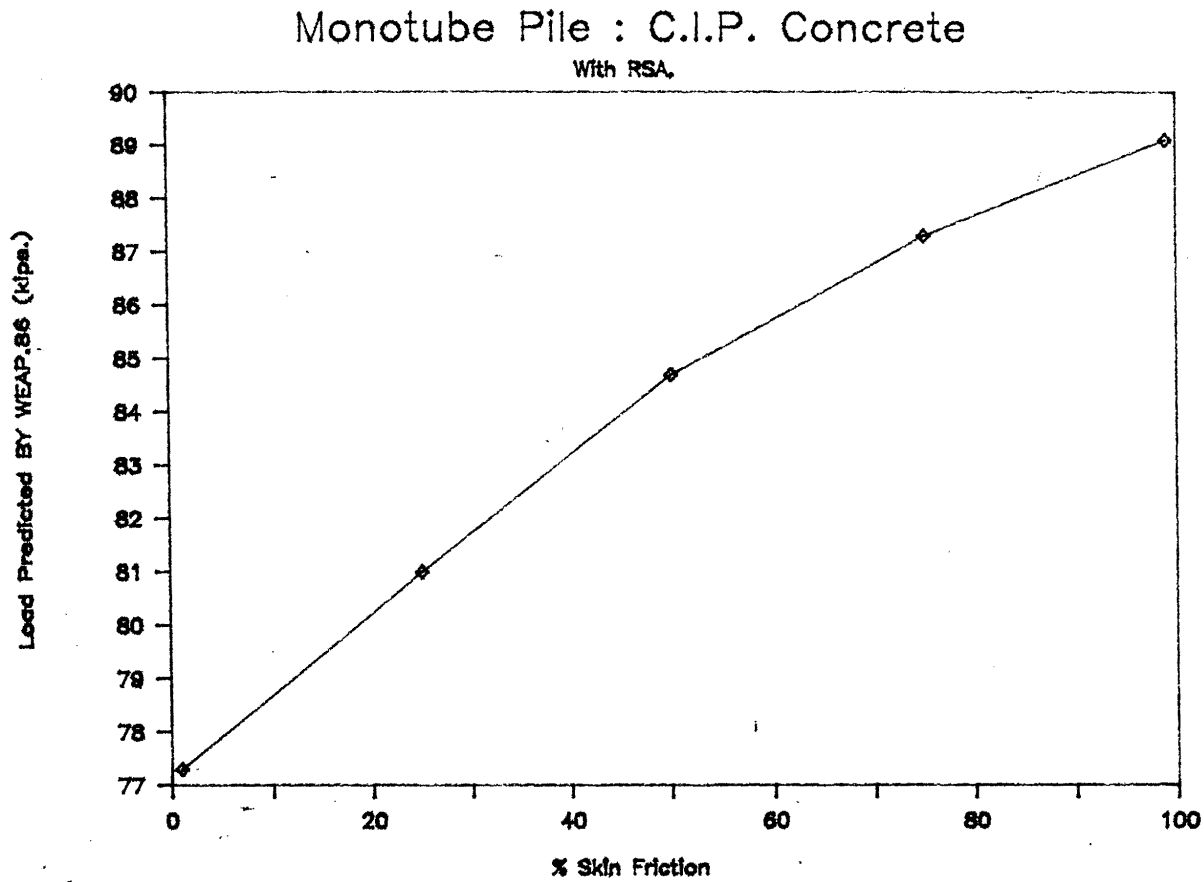

Figure 21

PHASE II

Stabilization of a Highway Embankment Using Steel Sheetpiling with Steel Batter Piles

I. OBJECTIVE

To monitor the performance of steel PZ-35 sheeting used in conjunction with steel HP 10 x 53 batter piles as a method of stabilizing a highway embankment against slope movement.

II. BACKGROUND

This project developed from a field condition that was declared an emergency in the Spring of 1987. The site, located on Route 66 in Portland, Conn., was experiencing recurring highway pavement settlement which inclinometers installed by Conn DOT showed to be progressive outward slope movements. This phenomenon has been occurring for the past several decades. Available information indicated that the greatest slope movements tend to occur during the spring high-water season, suggesting that pore pressures beneath the embankment may be a contributing factor. Another contributing factor may be the dynamic/vibratory loading caused by heavy vehicles passing the site.

The subsurface profile, as shown in Fig. 1, consists mainly of granular fill overlying peat, which rests on sand. Depth to bedrock varies from 20 feet (western edge of site) to 55 feet (eastern side). Bedrokc in primairly triassic sandstone of the portland formation. The presence of the organic peat exacerbates the problem.

CONNDOT engineers decided in May 1987 to attempt to stabilize the slope by structural means using steel sheeting supported

SUBJECT: Emergency Embankment Stabilization
Portland Rte. 66

Scale 1"=20' Typical Section - Approx Sta. 220+10

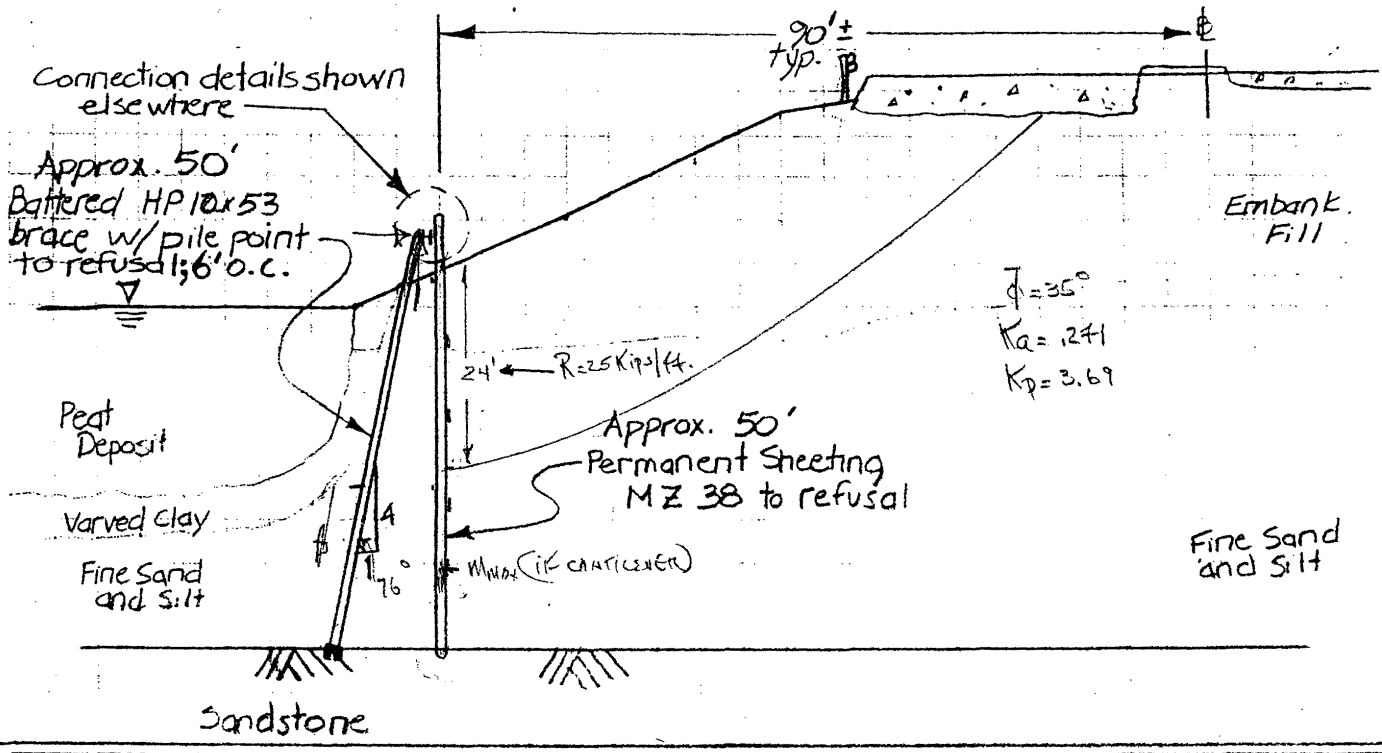

Scale 1"=40' Plan Treatment from Sta. 219+0 to Sta. 222+75
(Approx. 375 L.F.)

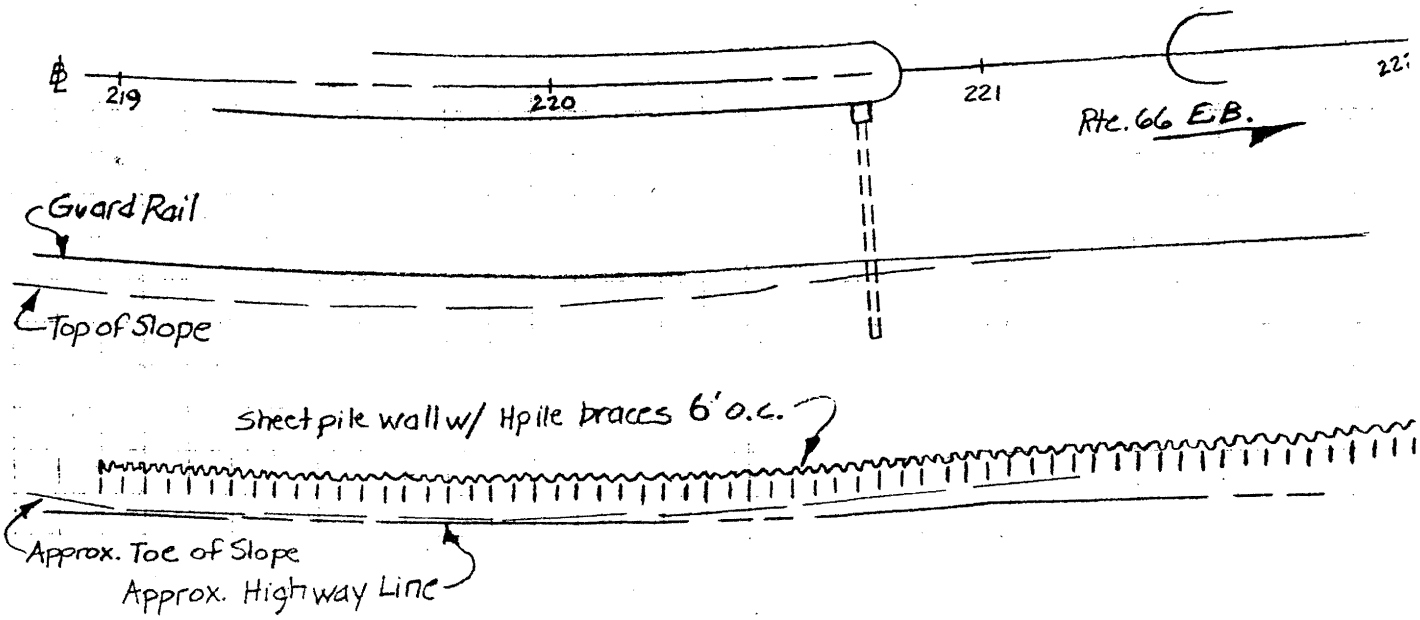

Figure 22

laterally by steel batter piles. UCONN personnel instrumented two sheetpile sections with strain gages to measure the strains induced in the sheeting. CONNDOT mounted slope indicator tubes at two other locations on the sheeting to monitor the deflection of the sheeting.

UCONN and CONNDOT staff implemented seperate instrumentation schemes which, would complement the evaluation of sheetpile performance.

III. INSTRUMENTATION PROGRAM

a. Underlying Theory

The inclinometer directly measures vertical slope with respect to a reference. The slopes along the vertical profile can be integrated, with an appropriate boundary condition, to give a deflection curve; or can be numerically differentiated using finite differences to obtain,

$$EIy'' = M, \text{ from small deflection beam theory,}$$

which can be compared with the strain gage data directly and implies that the spatial rate of change of slope is proportional to the internal bending moment at that section. However, accuracy and vertical positioning error makes this numerical integration approach only approximate at best.

b. UCONN Instrumentation Design and Construction

A strain gage instrumentation program was developed to determine the bending moment distribution along the vertical profile of the sheeting. Several challenging problems had to be addressed. The instrumentation had to withstand, a. impact driving by a Vulcan #1 pile driving hammer, b. a submerged environment below the ambient water table, c. potential damage by vandals.

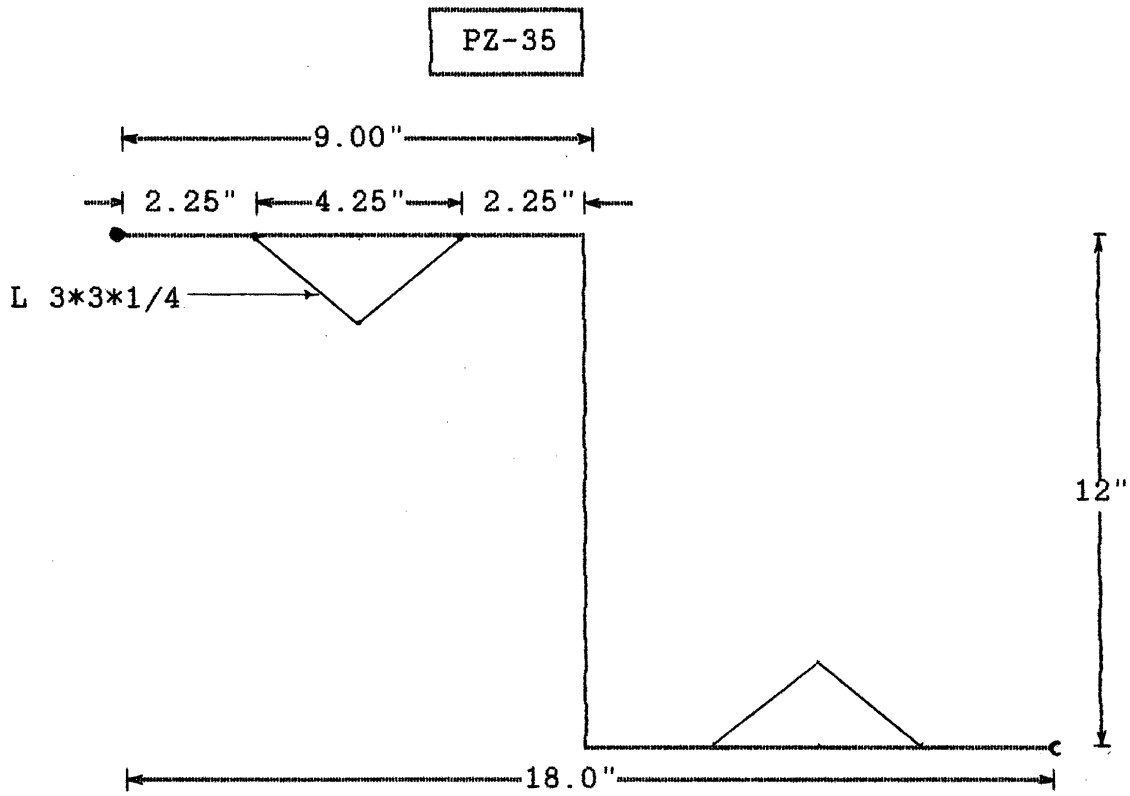

Figure 23a

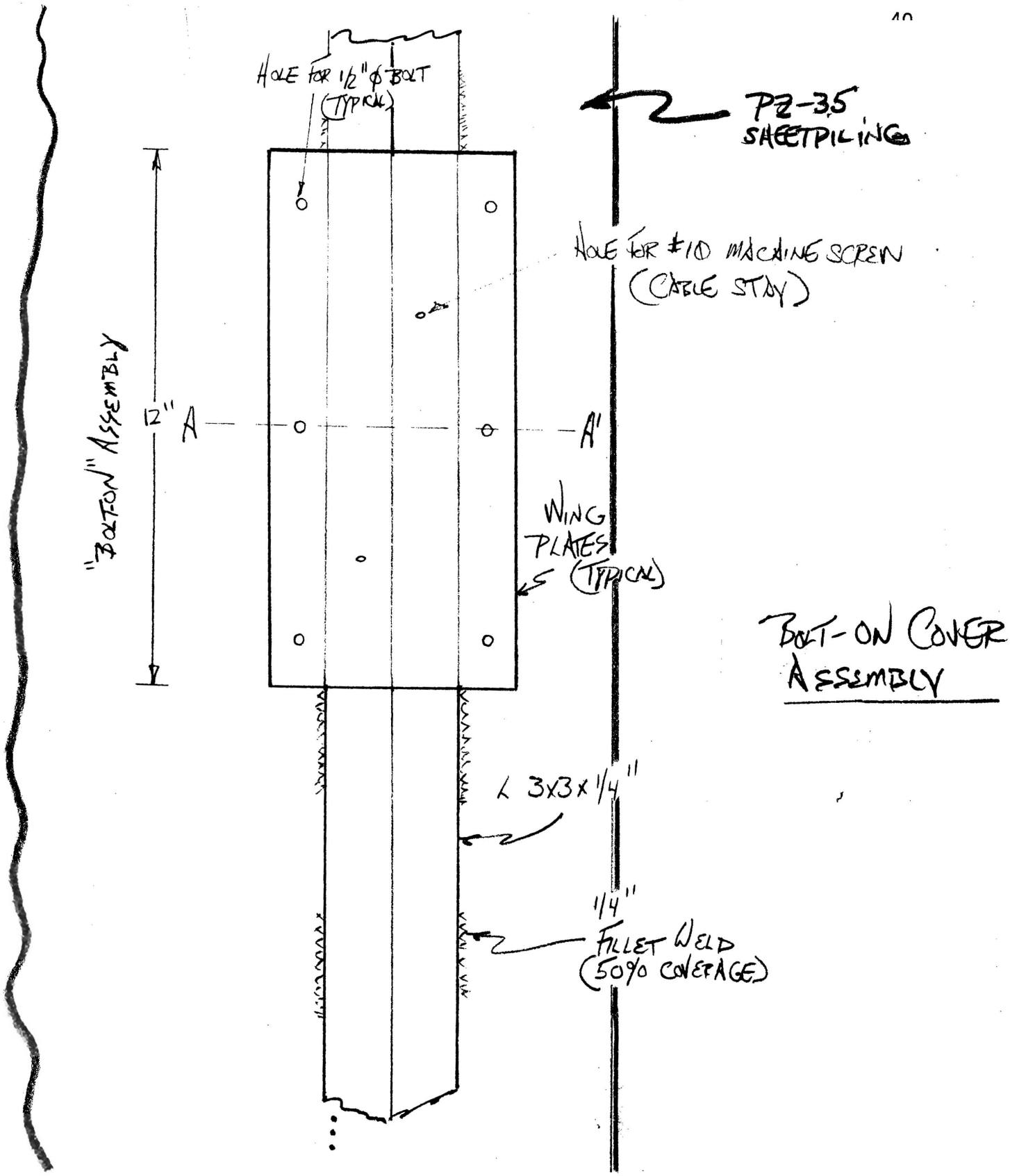
HOLE FOR 1/2" ϕ BOLT (TYPICAL)
PZ-35 SHEETPILING
HOLE FOR #10 MACHINE SCREW (CABLE STAY)
"BOLT-ON" ASSEMBLY
12"
A
A'
WING PLATES (TYPICAL)
BOLT-ON COVER ASSEMBLY
L 3x3x1/4"
1/4" FILLET WELD (50% COVERAGE)

Figure 23b

Advice was sought from Dr. J. Gartner of the University of Connecticut Mechanical Engineering Department, a specialist in instrumentation, and engineers at Micro-Measurements group of Raleigh, N.C. Electric resistance type strain-gages were selected for this project. In addition to gage selection and attachment to the pile, a means for protecting the instrumentation and its associated wiring required careful consideration. The cover scheme selected consisted of steel 3" x 3" angles placed longitudinally onto the flanges of the PZ-35 sheetpiling (Figure 23b). Ten foot long segments of the angle would be welded to a pile with 1 foot gaps left between them. Within these gaps would be placed the strain gage arrangment and protective coatings. Following gage installation, a 1 foot piece of steel angle would be bolted to the sheetpiling to protect the instrumentation assembly from physical damage during driving. Any attempt to exclude water from inside the angle sections would not be successful, hence individual waterproof coatings were applied to the gages instead.

The bonding of the gages to the steel piling was to be accomplished by spot-welding of the steel strain-gage backing to the piling, a task which was done in the field. A special layered application of sealants was applied to the area surrounding the gages after the necessary electrical connections were made to the strain gage (see Figure 24). Next, a steel 3x3" angle cover were bolted to the pile above the gages to help protect the instrumentation during pile driving operations.

Data Collection

Soon after pile installation, reference "zero" readings were taken on all strain gages using a Micromeasurements model P-3500

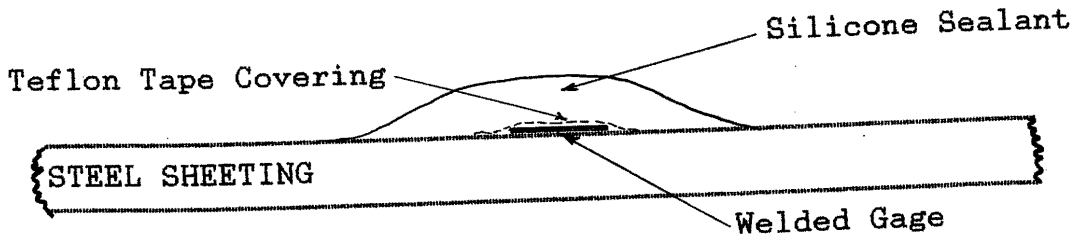

Figure 24

digital strain readout unit. Following the next several sets of observations, it was soon evident that the readings of the gages were eroneous. The problem was that the readout box would not give a stable reading; the reading drifted with time during measurement. The possibility of water or moisture getting to and possibly harming the gages was of primary concern. At this point, Mr. John Fickiet, Chief Electronic Technician at UCONN, was called in to assist in the investigation of this problem. Mr. Fickiet concluded that the design of the box, being of a high impedence input type, was picking up stray electromagnetic signals at the location and these signals were responsible for the drift problem. A low impedence type bridge, such as the older BLH type of wheatstone bridge circuitry was reccommended as a solution. Measurements taken with the BLH readout box indeed gave stable strain gage readings and was used exclusively thereafter.

Strain gages readings versus pile depth and gage readings versus elapsed time are shown in Figures 25 thru 32 for both the east and west instrumented sheetpiles.

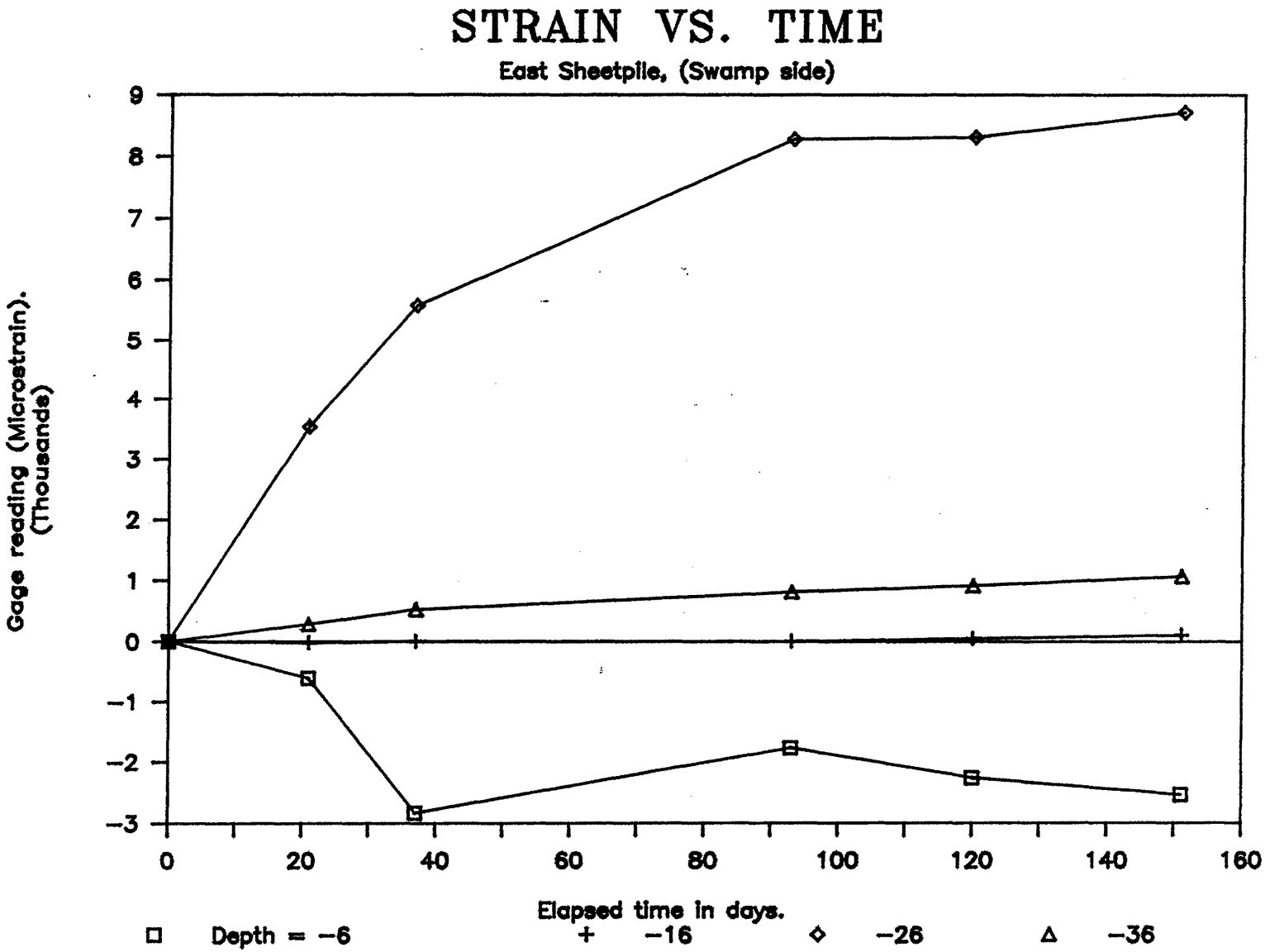
STRAIN VS. TIME
East Sheetpile, (Swamp side)
Gage reading (Microstrain). (Thousands)
9
8
7
6
5
4
3
2
1
0
−1
−2
−3
0
20
40
60
80
100
120
140
160
Elapsed time in days.
Depth = −6
−16
−26
−36

Figure 25

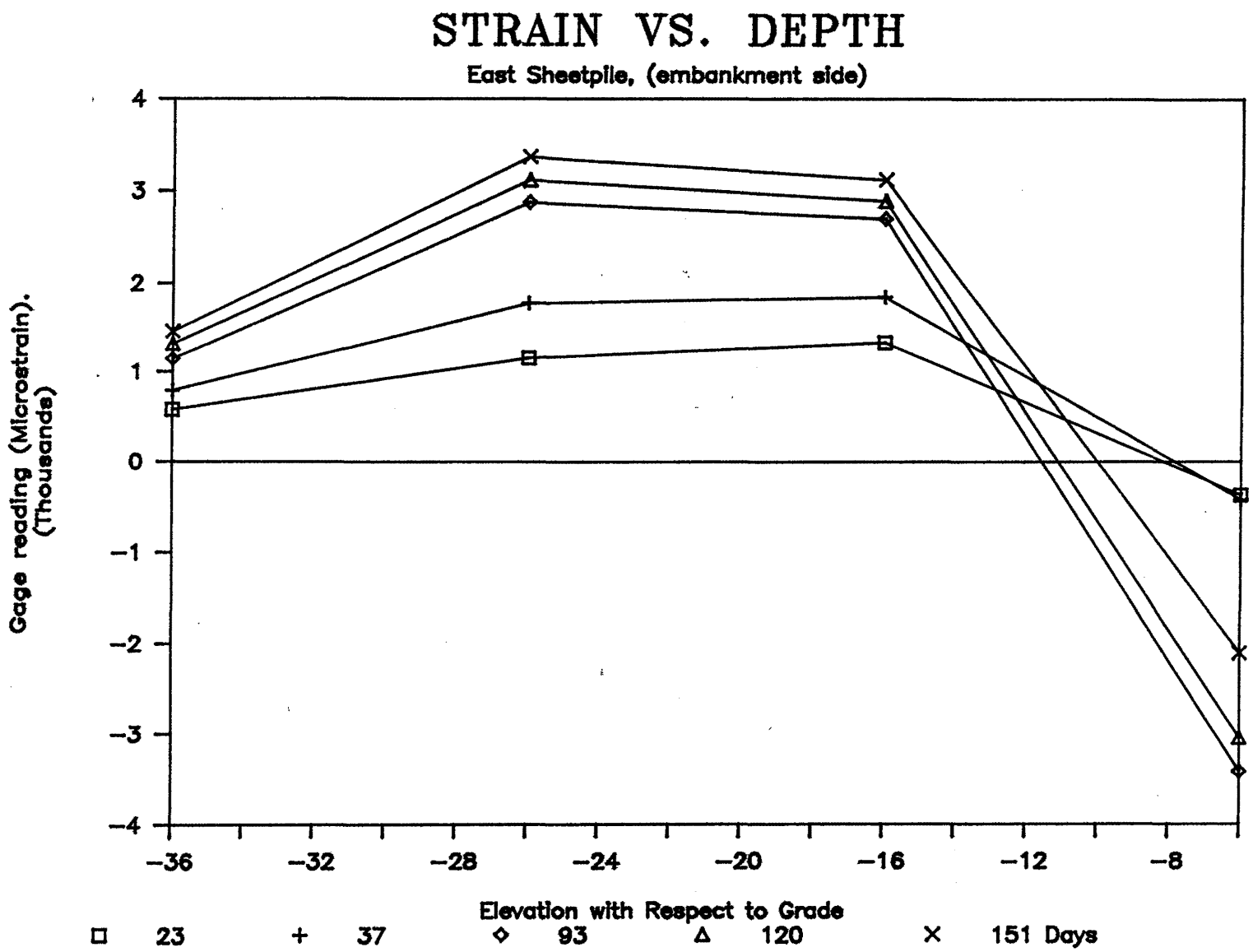
STRAIN VS. DEPTH
East Sheetpile, (embankment side)
Gage reading (Microstrain).
(Thousands)
4
3
2
1
0
−1
−2
−3
−4
−36
−32
−28
−24
−20
−16
−12
−8
Elevation with Respect to Grade
□ 23
+ 37
◇ 93
△ 120
× 151 Days

Figure 26

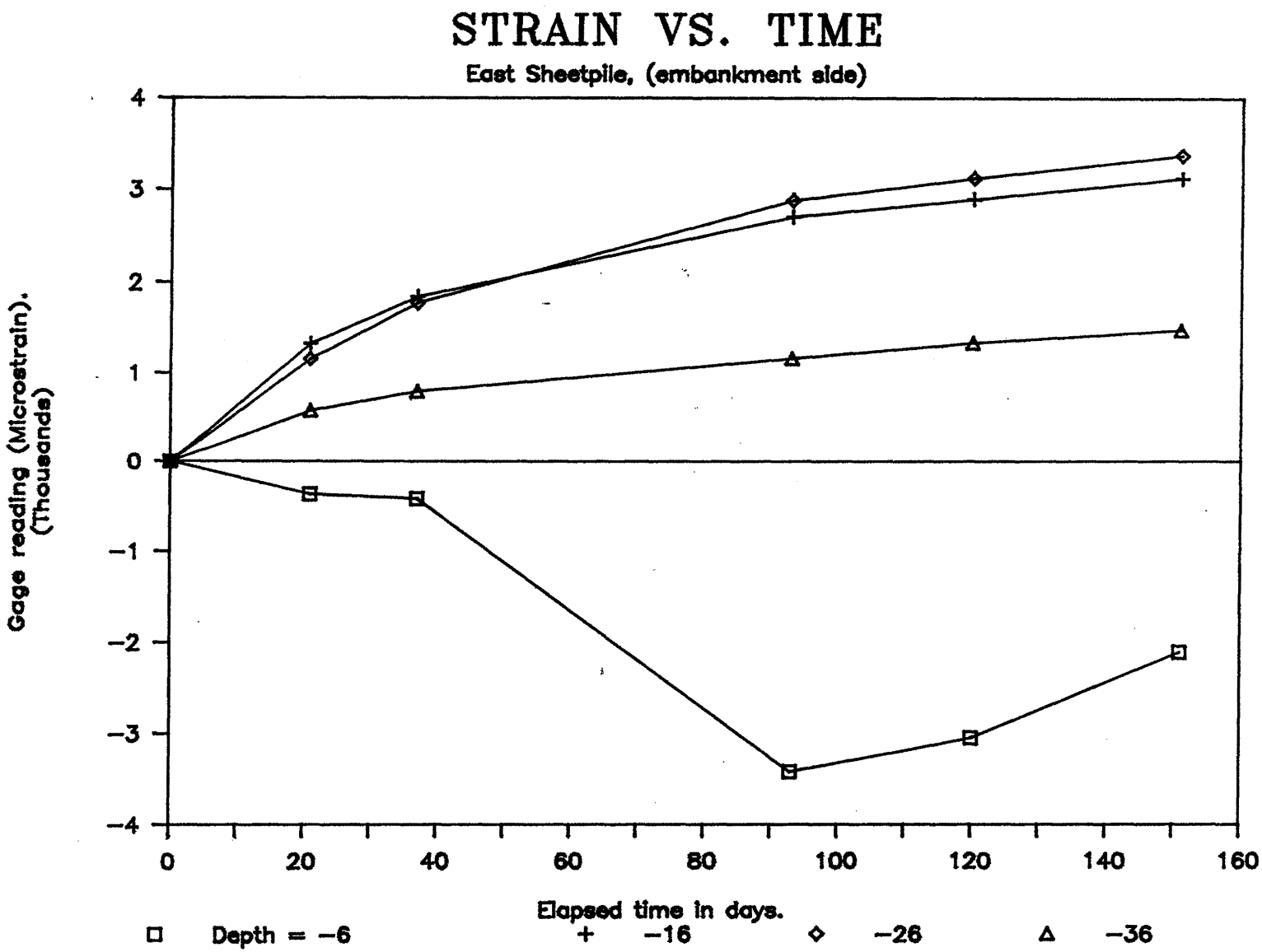
STRAIN VS. TIME
East Sheetpile, (embankment side)
Gage reading (Microstrain). (Thousands)
4
3
2
1
0
−1
−2
−3
−4
0
20
40
60
80
100
120
140
160
Elapsed time in days.
Depth = −6
−16
−26
−36

Figure 27

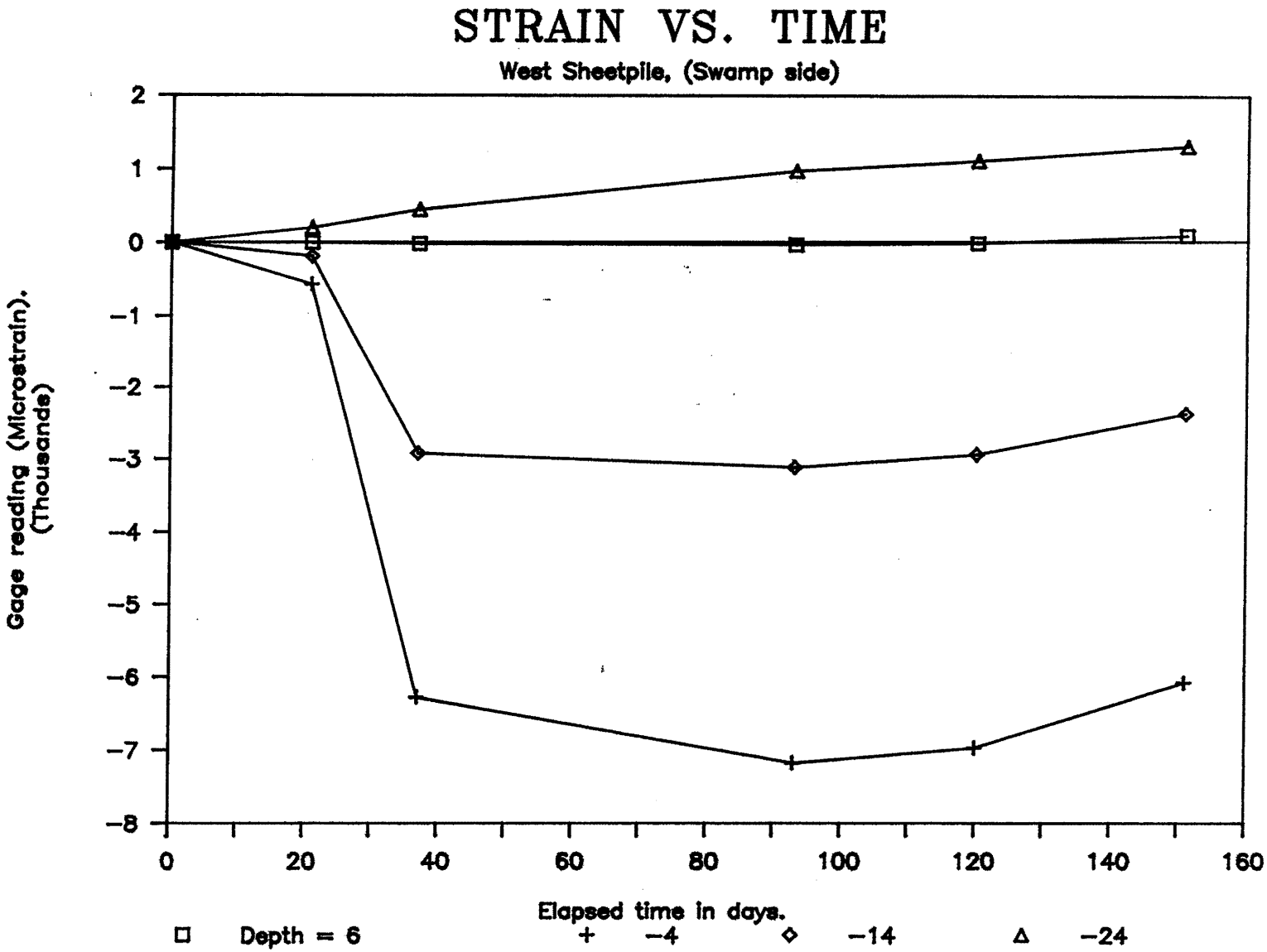
STRAIN VS. TIME
West Sheetpile, (Swamp side)
Gage reading (Microstrain).
(Thousands)
2
1
0
-1
-2
-3
-4
-5
-6
-7
-8
0
20
40
60
80
100
120
140
160
Elapsed time in days.
Depth = 6
-4
-14
-24

Figure 28

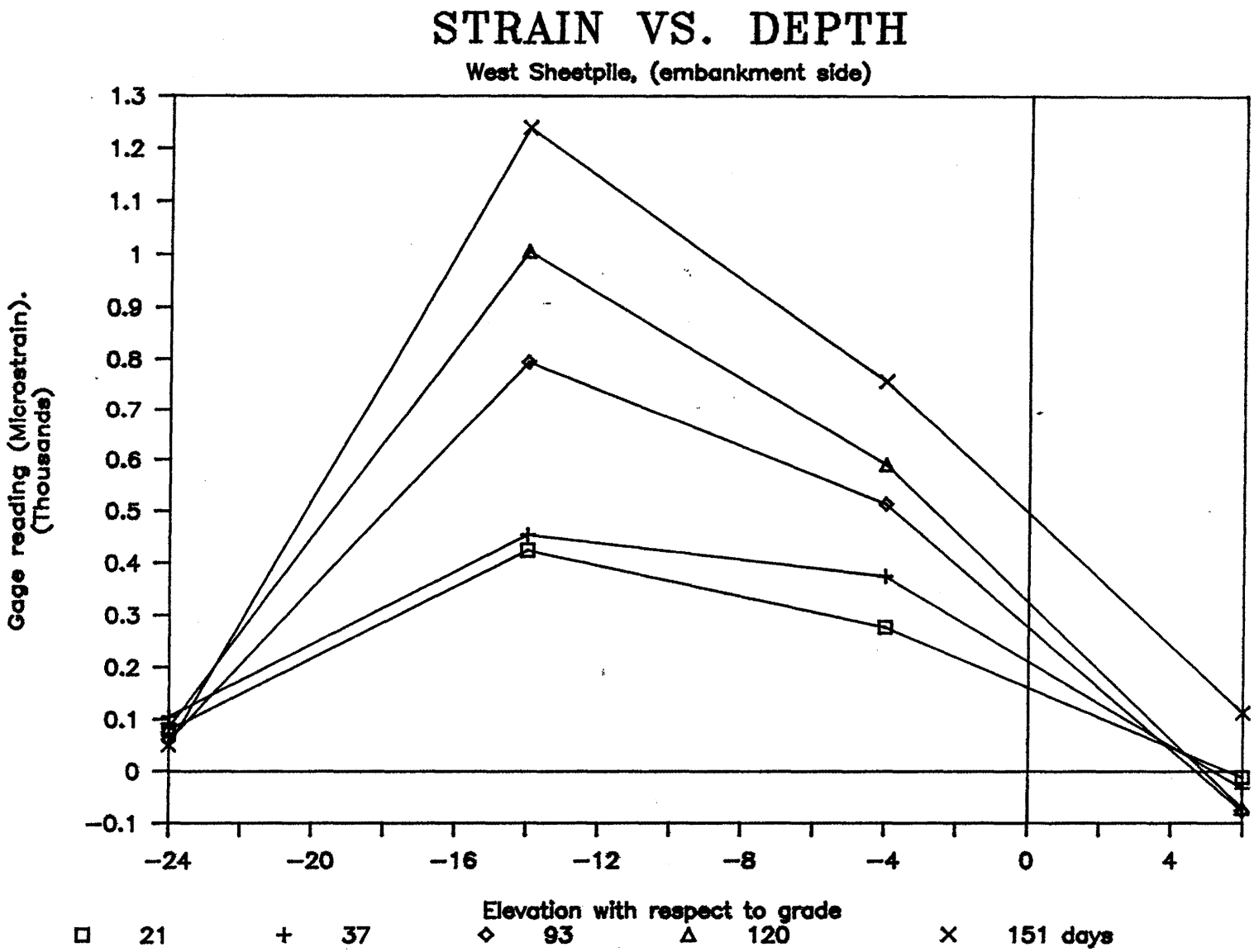
STRAIN VS. DEPTH
West Sheetpile, (embankment side)
Gage reading (Microstrain).
(Thousands)
1.3
1.2
1.1
1
0.9
0.8
0.7
0.6
0.5
0.4
0.3
0.2
0.1
0
-0.1
-24
-20
-16
-12
-8
-4
0
4
Elevation with respect to grade
21
37
93
120
151 days

Figure 29

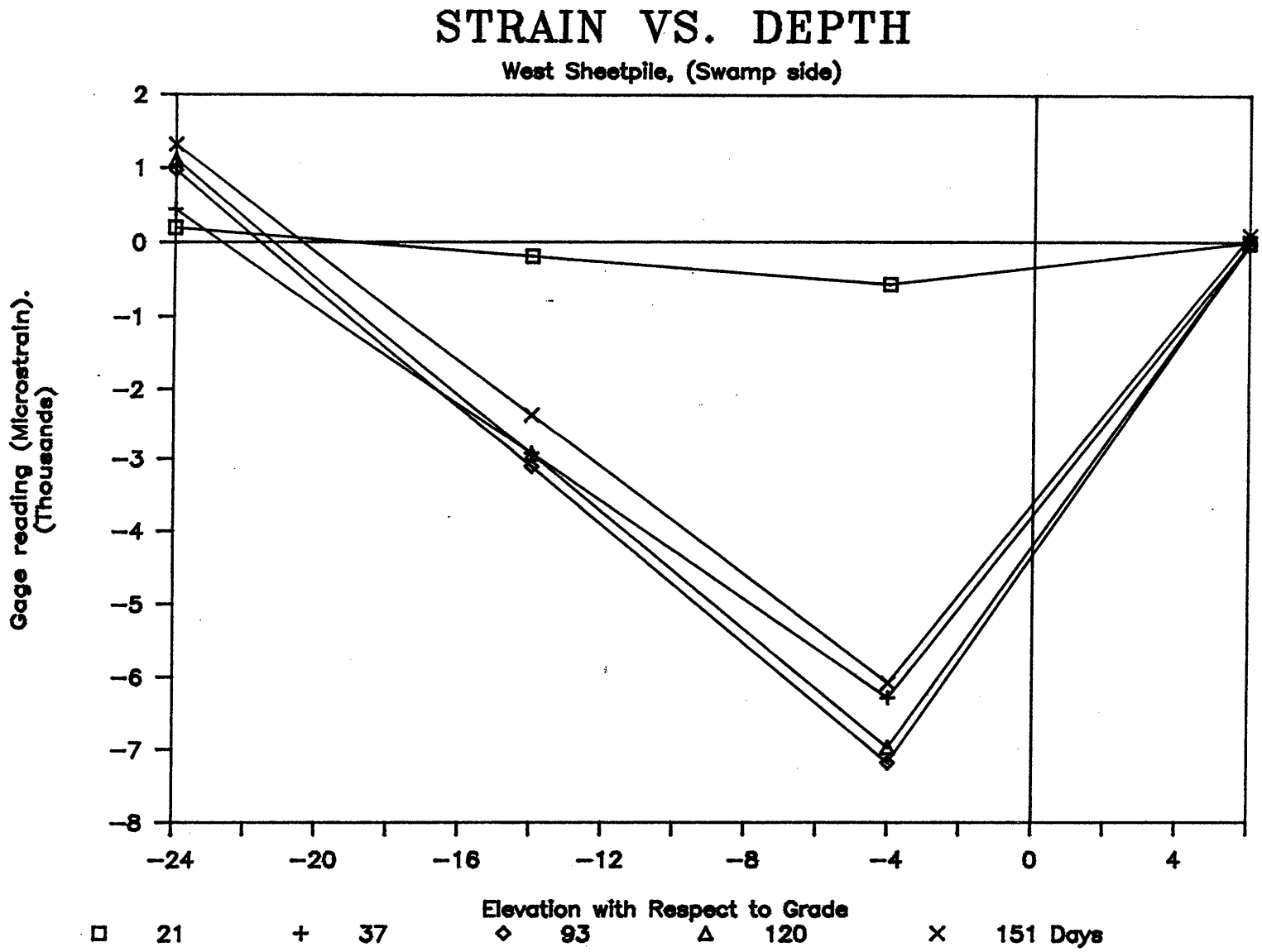
STRAIN VS. DEPTH
West Sheetpile, (Swamp side)
Gage reading (Microstrain).
(Thousands)
2
1
0
-1
-2
-3
-4
-5
-6
-7
-8
-24
-20
-16
-12
-8
-4
0
4
Elevation with Respect to Grade
21
37
93
120
151 Days

Figure 30

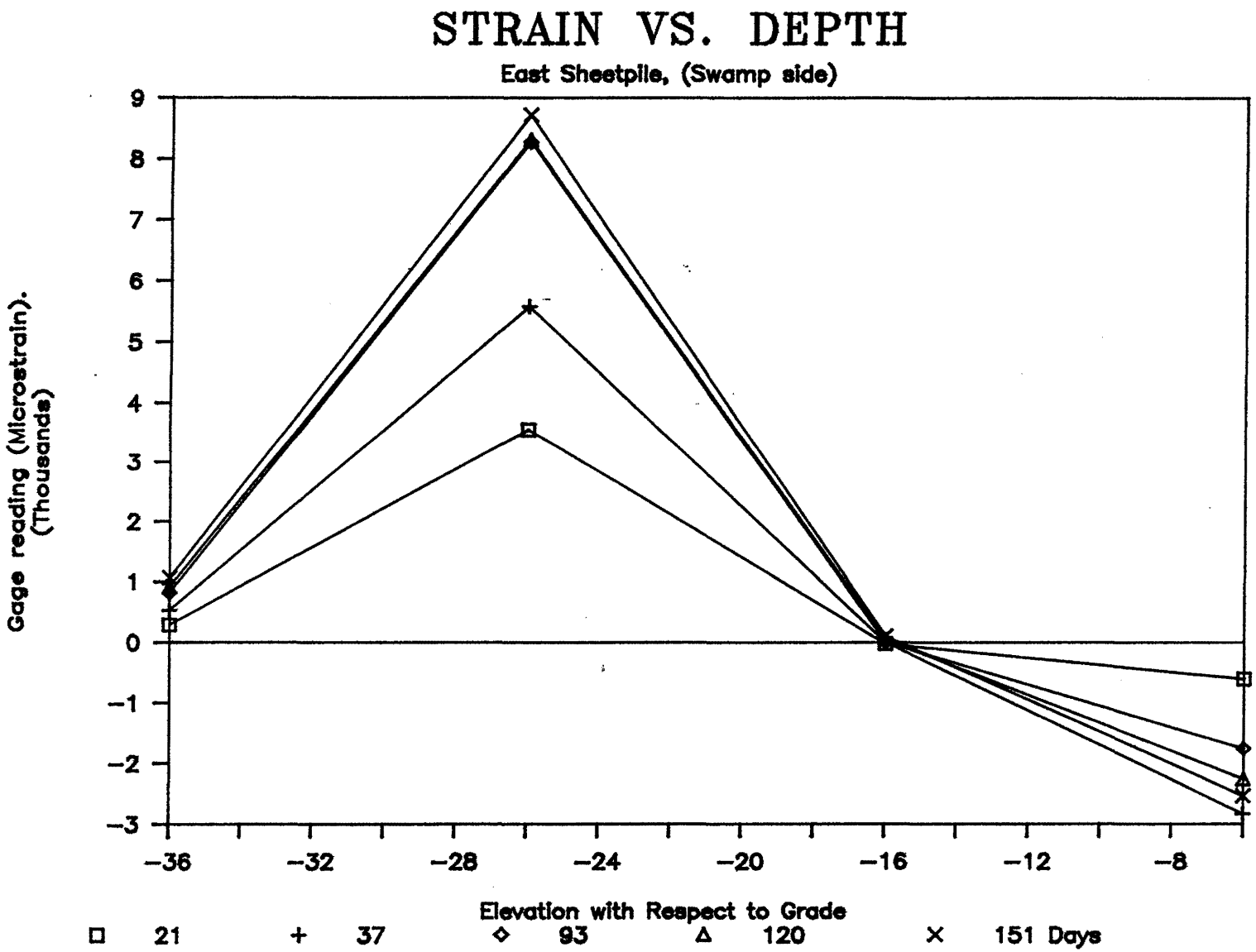
STRAIN VS. DEPTH
East Sheetpile, (Swamp side)
Gage reading (Microstrain).
(Thousands)
9
8
7
6
5
4
3
2
1
0
-1
-2
-3
-36
-32
-28
-24
-20
-16
-12
-8
Elevation with Reapect to Grade
21
37
93
120
151 Days

Figure 30

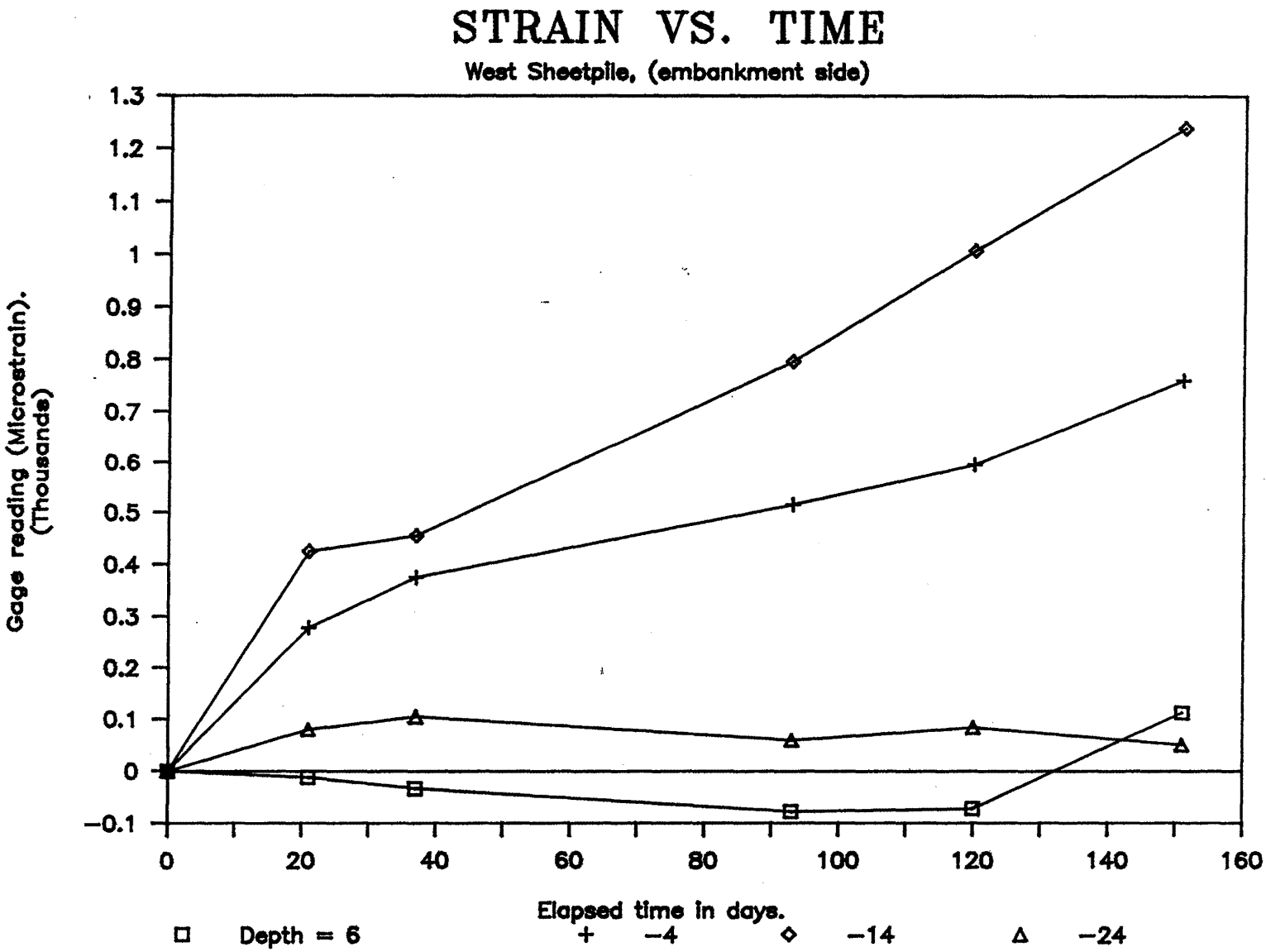
STRAIN VS. TIME
West Sheetpile, (embankment side)
Gage reading (Microstrain).
(Thousands)
1.3
1.2
1.1
1
0.9
0.8
0.7
0.6
0.5
0.4
0.3
0.2
0.1
0
-0.1
0
20
40
60
80
100
120
140
160
Elapsed time in days.
Depth = 6
-4
-14
-24

Figure 31

Calculations indicate that the maximum internal bending moment developed in the PZ-35 sheetpiling occurs at an elevation approximately 10 feet above the pile tip. In addition, the internal moment at the pile tip and pile butt appears to be quite small suggesting that conditions at these points approach those of pinned connections. Observation of the strain gage reading versus time plots (Figs. 25 thru 32) suggest that the pile-soil system, and slope has stabilized. This is further substantiated by observing that vertical settlement of the Route 66 pavement surface appears to have been arrested.

Bending moments were calculated by using linear-elastic assumptions together with simple beam theory; with

$M = S\ E\ \varepsilon_b$, where $\varepsilon_b = (\varepsilon_s - \varepsilon_e) / 2$

ε_s = strain on swamp side of sheeting

ε_e = strain on embankment side of sheeting

ε_b = strain due to bending

E = Young's modulus

S = section modulus of sheeting (per foot of wall)

M = internal moment in sheetpile

Independent inclinometer readings support the general shape of the moment versus depth curves. However; the magnitude of the bending moments do not agree with information obtained from inclinometer readings taken by ConnDOT personnel.

The measured bending moments obtained from the strain gages are several times higher than those back-calculated from the inclinomenter readings. Water infiltration onto the strain gages and associated electrical connections was investigated as a possible source of error. In light of the harsh environmental conditions

present, moisture may have worked its way onto the strain gages although the method of waterproofing recommended by the manufacture was used.

The University of Connecticut geotechnical engineering laboratories devised a simple laboratory experiment to measure the effect of moisture upon gage performance. The performance of a strain gage was measured by immersing the gage and associated electrical connections in a brackish water bath (to model in-situ conditions). The results, when compared to readings taken while the gage was dry, indicated that the microstrain readings were essentially the same after allowing for an initial drift period of several minutes duration for the gage to stabilize. Electrically, water acts as a parallel shunt resistance across the 120 ohm strain gage grid which makes the effective resistance of the gage slightly less than 120 ohms. Theoretically, this shunting effect should lessen the sensitivity (gage factor) of the strain gage, and apparent readings should be less than those actually occurring. However, as determined from the laboratory experiments, this effect is quite small. Therefore, water seepage can be tentatively ruled out as the primary reason for the abnormally high strain gage readings.

Conclusions

1. The maximum bending moment in the sheetpile appears occur about 10 feet from the bottom of the pile.
2. The magnitude of the maximum moment is uncertain as strain gage measurements and inclinometer data do not compare well.
3. The batter/sheetpile wall appears to have stabilized the slope against continued outward movement.
4. The Continued use of electrical resistance type strain gages in harsh environments is not recommended.

REFERENCES

1. Smith, E.A.L. (1960), "Pile Driving Analysis by the Wave Equation", J.S.M.F.D., A.S.C.E., Vol.86, SM4: pp. 35-61.

2. Kolsky, H. (1963), STRESS WAVES IN SOLIDS, Dover, New York.

3. Pochhammer, L. (1876), "J. Reine Angew" Math, Vol. 81, P. 324.

4. CAPWAP - Computer Analysis Program

5. Forehand, P.W. and Reese, J.L., (1964), "Prediction of Pile Capacity by the Wave Equation", J.S.M.F.D., A.S.C.E. Vol. 90, SM2, pp. 1-25.

6. Peck, R., Hansen, W. and Thornburn, T., (1974), FOUNDATION ENGINEERING, 2nd ed., New York, Wiley, p. 215.

7. Van der Veen, C., (1953), "The Bearing Capacity of a Pile", Proceedings of the Third Int. Conf. Soil Mech. Fed. Eng., Vol. 2, pp. 84-90.

8. Terzaghi, K., and Peck, R.B., (1967), Soil Mechanics in Engineering Practice, 2nd ed., Wiley, New York.

9. O'Neill, M., Unpublished information.

10. Holloway, D.M., Clough, G.W., and Vesic, A.S., "The Mechanics of Pile-Soil Interaction in Cohesionless Soils", Report for the Corp. of Engineers, Vicksburg, Miss., Dec., 1975.

REFERENCES

1. Smith, E.A.L. (1960), "Pile Driving Analysis by the Wave Equation", J.S.M.F.D., A.S.C.E., Vol.86, SM4: pp. 35-61.

2. Kolsky, H. (1963), STRESS WAVES IN SOLIDS, Dover, New York.

3. Pochhammer, L. (1876), "J. Reine Angew" Math, Vol. 81, P. 324.

4. CAPWAP - Computer Analysis Program

5. Forehand, P.W. and Reese, J.L., (1964), "Prediction of Pile Capacity by the Wave Equation", J.S.M.F.D., A.S.C.E. Vol. 90, SM2, pp. 1-25.

6. Peck, R., Hansen, W. and Thornburn, T., (1974), FOUNDATION ENGINEERING, 2nd ed., New York, Wiley, p. 215.

7. Van der Veen, C., (1953), "The Bearing Capacity of a Pile", Proceedings of the Third Int. Conf. Soil Mech. Fed. Eng., Vol. 2, pp. 84-90.

8. Terzaghi, K., and Peck, R.B., (1967), Soil Mechanics in Engineering Practice, 2nd ed., Wiley, New York.

9. O'Neill, M., Unpublished information.

10. Holloway, D.M., Clough, G.W., and Vesic, A.S., "The Mechanics of Pile-Soil Interaction in Cohesionless Soils", Report for the Corp. of Engineers, Vicksburg, Miss., Dec., 1975.